ASD TDR-62-31

ELASTOMERIC SEALS AND MATERIALS AT CRYOGENIC TEMPERATURES

D. H. Weitzel, R. F. Robbins, P. R. Ludtke, Y. Ohori, R. N. Herring

National Bureau of Standards
Cryogenic Engineering Laboratory
Boulder, Colorado

AERONAUTICAL SYSTEMS DIVISION

NOTICES

When Government drawings, specifications, or other data are used for any purpose other than in connection with a definitely related Government procurement operation, the United States Government thereby incurs no responsibility nor any obligation whatsoever; and the fact that the Government may have formulated, furnished, or in any way supplied the said drawings, specifications, or other data, is not to be regarded by implication or otherwise as in any manner licensing the holder or any other person or corporation, or conveying any rights or permission to manufacture, use, or sell any patented invention that may in any way be related thereto.

ASTIA release to OTS not authorized.

Qualified requesters may obtain copies of this report from the Armed Services Technical Information Agency, (ASTIA), Arlington Hall Station, Arlington 12, Virginia.

Copies of ASD Technical Reports and Technical Notes should not be returned to the Aeronautical Systems Division unless return is required by security considerations, contractual obligations, or notice on a specific document.

ASD TDR-62-31

ELASTOMERIC SEALS AND MATERIALS AT CRYOGENIC TEMPERATURES

D. H. Weitzel, R. F. Robbins, P. R. Ludtke, Y. Ohori, R. N. Herring

National Bureau of Standards
Cryogenic Engineering Laboratory
Boulder, Colorado

Directorate of Materials and Processes
Contract No. AF 33(616)-61-04
Project No. 7340

AERONAUTICAL SYSTEMS DIVISION
AIR FORCE SYSTEMS COMMAND
UNITED STATES AIR FORCE
WRIGHT PATTERSON AIR FORCE BASE, OHIO

FOREWORD

This report was prepared by the National Bureau of Standards under USAF Contract No. 33(616)-61-04. This contract was initiated under Project No. 7340, "Nonmetallic and Composite Materials", Task No. 73405, "Elastomeric and Compliant Materials". The work was administered under the direction of Directorate of Materials and Processes, Deputy for Technology, Aeronautical Systems Division, with Mr. Roger Headrick acting as Project Engineer.

This report covers work conducted from November,1960 to November, 1961.

ABSTRACT

This research deals with investigations of elastomeric polymers, with particular emphasis on their usefulness as seals at cryogenic temperatures. O-ring seals utilizing various flange configurations have been extensively evaluated at temperatures between 76 and 300°K. A supporting program of property measurements includes thermal expansivities, shear and compression modulus, differential thermal analysis, and the force-temperature effects of prestressed elastomers. O-rings and other specimens have been prepared and supplied by Aeronautical Systems Division.

PUBLICATION REVIEW

This Report has been reviewed and is approved.

FOR THE COMMANDER:

J. M. Kelble, Chief
Elastomers and Coatings Branch
Non-Metallic Materials Laboratory
Directorate of Materials and Processes

TABLE OF CONTENTS

Table of Contents (continued)

LIST OF FIGURES

List of Figures (continued)

LIST OF TABLES

Introduction

This research is concerned with the study of elastomeric polymers for applications at cryogenic temperatures. Emphasis has been on the development of effective seals for use at very low temperatures, and principles for this purpose have been established. An increasing emphasis on measurement of physical properties has accompanied the seal testing. This phase of the program should expand its usefulness to other applications as well as contribute to the understanding of basic polymer structure and compounding.

1. Static Seals

A fixture for testing highly compressed elastomer o-ring seals is shown in Figure 1. This fixture and the seal test procedure have been described in previous reports [1]. It has been found that standard commercial o-rings of 1/8 inch cross section diameter can be used to make excellent seals at cryogenic temperatures.

It has also been shown by previous work[1] that thin flat gaskets of poly (ethylene terephthalate) or nylon make excellent cryogenic seals with relatively low flange loads. The key to success in this case is the method of applying sealing force to the gasket, and consists essentially of setting up a narrow ring of highly concentrated stress to form the seal.

1.1 O-Ring Seals

The elastomer o-ring concept has been explored in two additional ways. These are the use of o-rings of small cross section in the tongue and groove flange design and the use of o-rings between flat plates. O-rings of 1/16 inch cross section diameter have made satisfactory seals in a tongue and groove flange design and required about half as much bolt loading as 1/8 inch o-rings of the same material. Thus one of the principal disadvantages of the original seals of this design can be substantially reduced.

The original tongue and groove flange design was dimensioned to closely confine the o-ring at the end of the linear compression, and then subject the confined elastomer to about 5% volume compression. This required close machining tolerances in the flange construction, and high bolt loads at the end of the compression. Although the resulting seal is very reliable, and can be made with a large number of elastomer compounds, it has now been found that some of the elastomers make satisfactory seals without lateral or "side" confinement.

Manuscript released by the authors January 1962 for publication as an ASD Technical Documentary Report.

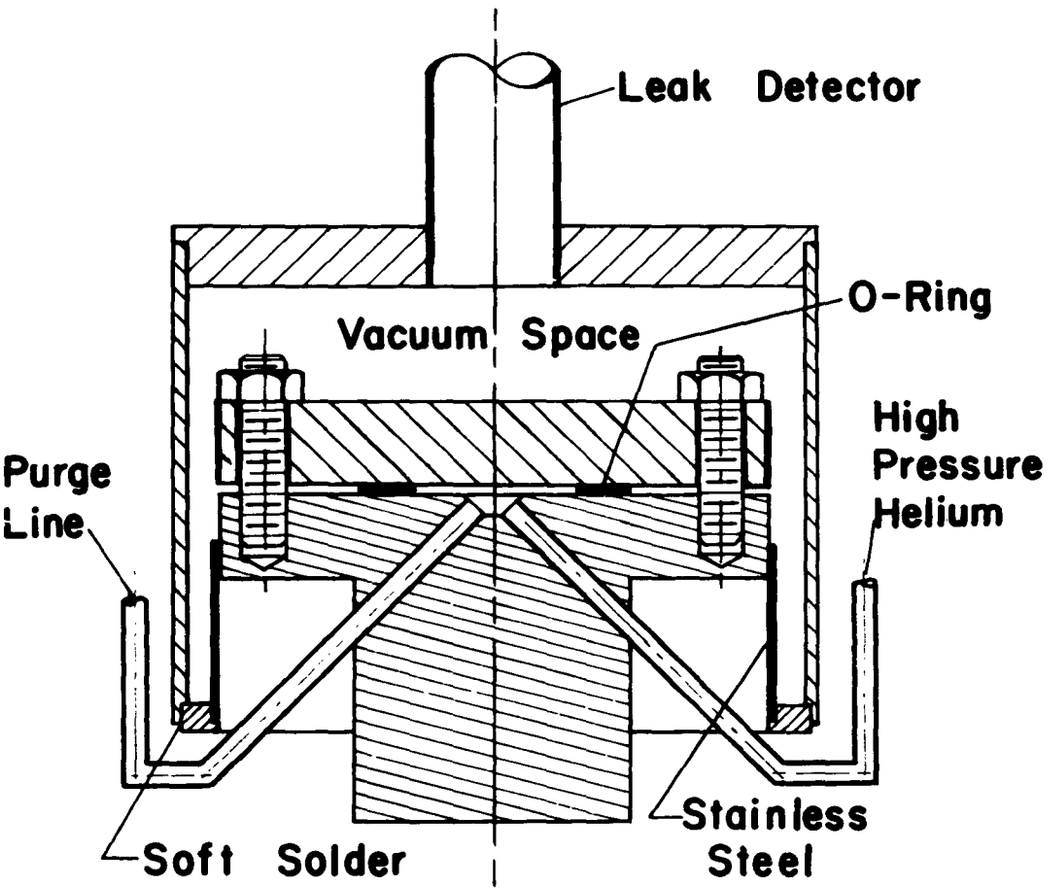

Fig. 1· O-Ring Seal Test Jig .

There are several advantages to this modification: (1) the flange loading is about half that required for a confined o-ring of the same cross section; (2) the flanges require a minimum of machining and there are no close machining tolerances; and (3) the surface finish of the flanges is not critical - in fact, a somewhat rough machine finish is advantageous since it helps prevent excessive flow of the otherwise unconfined elastomer.

Minimum bolt loading will be required to make the seal if an o-ring of minimum cross-section is compressed between ungrooved flat flanges. A preliminary study of this type of seal was made by compressing 1-inch diameter by 1/16-inch thick o-rings between smooth surfaces. The fixture used was that shown in Figure 1, with the tongue and groove machined off to form flat surfaces.

Results of this testing are shown in Table 1. These tests were not exhaustive, but two commercial elastomer compounds and a common plastic made excellent seals with little or no material failure when tested at 76°K and 1000 psig. There is little doubt that further experimentation would show that other polymer compounds can be used to make successful seals of this kind. Further testing of similar seals will be described in the next section.

The top flange used for the tests shown in Table 1 was 3/8-inch thick stainless steel, and compression of the 1-inch diameter o-ring was by means of six 3/8-inch steel studs on a 2 1/4-inch bolt circle. This construction is quite rigid, considering the size of the o-rings used, but flange loading was in most cases high enough to cause significant strains in the metal parts. This distortion of flanges and studs "spring loads" the o-ring so that differential shrinkage during cooldown is less likely to separate the brittle elastomer from the confining flanges. A more severe test of the o-ring seals would be one in which this spring loading effect of bolts and flanges has been eliminated.

1.2 Heavy Plate Seal Tests

Shown in Figure 2 is a heavy plate fixture which was designed to test o-ring seals without the complications introduced by stretching of bolts or flexing of flanges. The flanges were made of 2 inch thick stainless steel, and compression was by means of six 3/4 inch diameter stainless steel studs. A machined depression in the center of one flange allowed the studs to be pulled up tight for metal-to-metal contact after the o-ring had been compressed the desired amount.

Basic Type	Polymer	Compound No. *	Shore A Hardness	Bolt Torque (ft-lb)	Compression (%)	Material Failure	Seal Failure	Test Pressure (psig)	Final or Failure Temp. (^{o}K)	O-Ring Width (in)
Chlorosulfonated Polyethylene	Chlorosulfonated Polyethylene	921	65	10-15	85	No	No	1000	76	.070
Natural	Natural Rubber	634	50	16-17	90	No	Yes	50	86	.070
Buna N (Nitrile)	Butadiene-acrylonitrile	427	50	20-25	90	Severe	No	1000	76	.070
Neoprene	Chloroprene	307	50	10-15	94	No	No	1000	76	.070
Butyl	Isobutylene-isoprene	805	40	5-10	85	No	Yes	50	137	.070
Buna N (Nitrile)	Butadiene-acrylonitrile	228	50	10	86	No	No	250	76	.070
Government Rubber-Styrene	Butadiene-styrene	132	50	5	85	No	Yes	50	158	.070
Polysulfide	Polysulfide	501	70	5-10	85	Severe	Yes	125	155	.070
Fluorocarbon	Polytetrafluoro-ethylene			25	90	Slight	No	1000	76	.100
Fluorocarbon	Polytetrafluoro-ethylene-coated stainless steel			5	50	No	No	125	76	.094

* "Parco" brand compounds supplied by Plastic and Rubber Products Company

Table 1. FLAT FLANGE SEAL TESTS

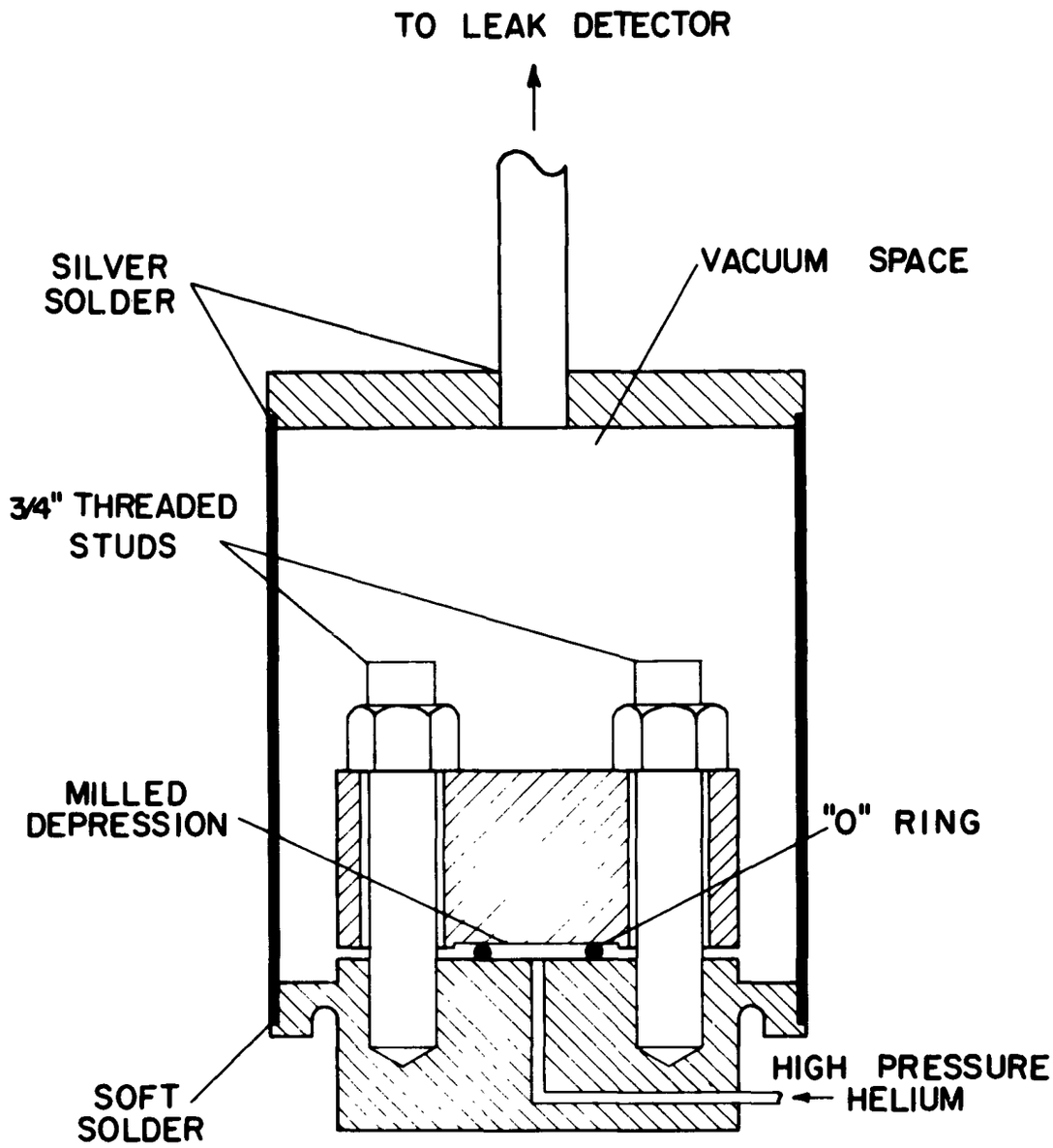

FIG. 2. Heavy Flange O-Ring Tester

The amount of squeeze (percent compression) of the o-ring was increased by placing thin metal discs in the bottom of the depression, or decreased by placing a thin metal insert between the flanges at the bolt circle. All surfaces were given a normal machine finish.

With this heavy fixture, flexing of flanges was reduced to a negligible level through overdesign, and stress due to stretching of bolts was absorbed by metal-to-metal contact at the bolt circle. There remained the spring loading which results from compression of the steel flange faces. For high squeezes the compression of metal above the o-ring was sufficient to result in a slight permanent depression showing that the elastic limit of stainless steel had been exceeded in the region immediately adjacent to the ring. There appeared to be no easy way to design around this effect, and it is present in all our tests. The amount of spring loading obtained in this way is very small, however, in comparison with that experienced with flanges of practical thickness.

It should be emphasized, of course, that spring loading inherent in most flange designs contributes to the effectiveness of o-ring seals for cryogenic use and thus should be utilized rather than eliminated. Since this has been a largely unknown and variable parameter, however, it has complicated the study of o-ring seal performance. Results with the oversize jig, even without strain gauge instrumentation, has been quite informative. These results are summarized in Table 2.

Commercial and Aeronautical Systems Division compounds* of chlorosulfonated polyethylene (hereafter called c.s.p.), natural rubber, vinylidene fluoride/perfluoropropylene (hereafter called v.f.p.), and neoprene, all of which have been good seal materials in previous functional tests, were tested in the heavy jig. The o-rings, in .070 and .140-inch thicknesses, were tested at progressively higher compressions until either a satisfactory low temperature seal was achieved or severe material failure resulted. Neither v.f.p. nor c.s.p. performed well under the conditions of this test. Apparently a certain amount of spring loading is required before either of these materials, as compounded in our samples, will make satisfactory cryogenic seals. The compounds based on natural rubber and neoprene, on the other hand, performed quite well without spring loading.

* For compounding recipes and original physical properties of A.S.D. materials see Table 3.

Compound	Shore A Hardness	O-Ring Width (in)	Percent Compression	Maximum Pressure (psi)	Material Failure	Pressure Cycles	Temp. Cycles	Seal Failure	Final or Failure Temp. (°K)	Test Number
Commercial c.s.p.[1]	65	.070	70	100	None	0	0	Yes	153	1-H
ditto	65	.070	84	100	Severe	0	0	Yes	295	3-H
Commercial v.f.p.[2]	80	.070	70	100	None	0	0	Yes	280	7-H
ditto	80	.070	78	100	None	0	0	Yes	185	8-H
ditto	80	.070	88	1250	Severe	20	2	No	81	13-H
Commercial Natural	50	.070	84	100	None	1	1	Yes*	93	4-H
ditto	50	.070	88	1250	Slight	50	2	No	76-93	9-H
ditto	50	.070	91	1250	Severe	50	3	No	76-93	5-H
Commercial Neoprene	50	.070	84	100	None	0	0	Yes	128	12-H
ditto	50	.070	88	1250	Slight	20	2	No	76-93	11-H
ditto	50	.070	91	1250	Severe	50	2	No	76-93	10-H
Natural Rubber										
A.S.D. Comp. 8A	65	.140	70	100	None	0	0	Yes	153	3-P
ditto	65	.140	75	100	None	0	0	Yes	128	4-P
ditto	65	.140	80	100	Slight	0	0	Yes	122	5-P
ditto	65	.140	85	1250	Severe	0	0	No	76-93	13-P
Commercial Natural	50	.140	75	100	None	0	0	Yes	142	9-P
ditto	50	.140	80	100	None	0	0	Yes	142	10-P
ditto	50	.140	87	1250	Severe	30	2	No	76-93	11-P
Neoprene										
A.S.D. Comp. 8B	85	.140	70	1000	None	10	0	Yes**	93	1-P
ditto	85	.140	75	1250	Severe	30	2	No	76-93	2-P
Commercial Neoprene	50	.140	70	100	None	0	0	Yes	173	6-P
ditto	50	.140	75	100	None	0	0	Yes	135	7-P
ditto	50	.140	80	100	None	0	0	Yes	138	8-P
ditto	50	.140	85	1250	Severe	30	2	No	76-93	12-P
Commercial c.s.p.	65	.140	85	100	Severe	0	0	Yes	138	2-H
A.S.D. Comp. 8D(v.f.p.)	80	.140	70	100	Severe	0	0	Yes	173	16-P
ditto	80	.140	75	100	Severe	0	0	Yes	153	14-P
ditto	80	.140	80	100	Severe	0	0	Yes	210	15-P

(1) chlorosulfonated polyethylene

(2) vinylidene fluoride/perfluoropropylene

* tested cold after 3 days compressed at room temperature

** upon removal from bath and jarring on floor

Table 2.. HEAVY FLANGE TEST RESULTS

ASD No	Polymer	Estimated Monomer Ratio	Recipe		Original Properties			
					Tensile Strength (PSI)	Ultimate Elongation (%)	Hardness (Shore A)	Compression Set* (%)
Group IV								
8A	Natural Rubber		Polymer (Smoked Sheet)	100	2200	350	65	10
			Stearic Acid	3				
			Zinc Oxide	5				
			N-cyclohexyl -2-benzothiazole sulfenamide	0.6				
			Sulfur	2.75				
			HAF Carbon Black	50				
			Polymerized Trimethyl dihydroquinoline	1				
			Cure 15 min at 310°F					
8B	Chloroprene		Polymer (WRT)	100	2200	175	85	11
			Stearic Acid	5				
			Zinc Oxide	5				
			Magnesium Oxide (ELC)	4				
			HMF Carbon Black	50				
			Na 22	0.5				
			Cure 20 min at 310°F					
Group VIII								
8C	Chlorosulfonated Polyethylene		Polymer	100	2080	150	90	36
			Magnesium Oxide	10				
			Hexamethylene Diamine Carbamate	1				
			Pentaerythritol	5				
			"Magcarb W"	10				
			HMF Carbon Black	5				
			Cure 20 min at 310°F					

* 50% Compression, 90 hrs at room temperature.

Table 3. RECIPES AND PROPERTIES OF ASD MATERIALS USED IN HEAVY FLANGE, THERMAL EXPANSION, AND GLASSY TRANSITION POINT TESTS

ASD No	Polymer	Estimated Monomer Ratio	Recipe		Original Properties			
					Tensile Strength (PSI)	Ultimate Elongation (%)	Hardness (Shore A)	Compression Set* (%)
Group 1								
8D	Vinylidene fluoride and Perfluoropropylene	70/30	Polymer	100	2900	190	80	50
			Magnesium Oxide	20				
			Hexamethylene Diamine Carbamate	1.3				
			MT Carbon Black	25				
			Cure 20 min at 280°F					
			Post cure 16 hr at 400°F					
12B	Ditto	70/30	Additives Ditto 8D		2840	330	80	73
			Cure 20 min at 310°F					
			Post Cure 16 hr at 400°F					
12C	Ditto	70/30	Ditto		2760	210	80	64.5
12A	Vinylidene fluoride and Perfluoropropylene and (Third Monomer Unknown)	Terpolymer	Ditto		3180	310	75	18
12E	Vinylidene fluoride and Monochlorotrifluoro ethylene	70/30	Polymer	100	1000	650	80	80
			Zinc Oxide	5				
			EP Carbon Black	10				
			Dibasic Lead Phosphite	5				
			Hexamethylene Diamine Carbamate	1.3				
			Cure 30 min at 310°F					
			Post cure 16 hrs at 300°F					
12D	Ditto	50/50	Polymer	100	1315	615	75	70
			Zinc Oxide	5				
			"Hi Sil"	15				
			Dibasic Lead Phosphite	5				
			Benzoyl Peroxide	3				
			Cure 20 min at 280°F					
			Post cure 16 hrs at 300°F					

* 50% Compression, 90 hrs at room temperature.

Table 3 (Continued) RECIPES AND PROPERTIES OF ASD MATERIALS USED IN HEAVY FLANGE, THERMAL EXPANSION, AND GLASSY TRANSITION POINT TESTS

In .070-inch width the latter two materials showed little or no material failure at 88% true compression, and made reliable high vacuum seals at temperatures from room temperature to between 76 and 93°K, and at pressures to 1250 psig. Satisfactory seals were also obtained with these compounds in .140-inch width o-rings, but only after compression reached the point of severe material failure.

From these tests we can conclude that standard compounds of neoprene and natural rubber will make satisfactory seals for use at cryogenic temperatures, with little or no spring loading required, if .070-inch o-rings are compressed to just short of material failure. Compression beyond material failure does not necessarily mean that the seal will leak but this requires more flange loading than necessary and of course destroys the o-ring.

The pressure and temperature cycles indicated in Table 2 were introduced to provide a more severe test of seal reliability. Pressure cycling was done after the seal was cold, and consisted of 10 cycles between 1 atmosphere and the maximum pressure shown in Table 2. The jig was cooled in liquid nitrogen for 2 hours at 100 psig, which brought the temperature of the seal to about 97°K. After this the pressure was raised to maximum and cooling continued for 30 to 60 minutes. If the seal was tight the pressure was reduced and the jig warmed in hot water, which completed one temperature cycle. The second cooldown was with 1000 psig on the seal, and this was raised to 1250 psig after 2 to 3 hours in liquid nitrogen.

In general, neither pressure nor temperature cycling caused an initially satisfactory seal to leak. The seal in test 4-H leaked when cooled down a second time after being assembled for a week-end. This indicates that relaxation may be an additional factor which should be investigated. In test 1-P the seal was tight through 10 pressure cycles and while cold at 1000 psig, but began to leak when removed from the bath and jarred against the concrete floor. It is interesting to note that every seal which held at 100 psig was also satisfactory at 1000 or 1250 psig.

Perhaps the greatest value of this series of tests is that it makes possible some further differentiation among materials and o-ring sizes which have passed all previous tests. Thus it appears now that compounds of natural rubber and neoprene may make reliable cryogenic seals under more severe conditions than compounds of v.f.p. or c.s.p. It is also quite clearly indicated that the .070-inch o-ring width is to be preferred over the larger .140-inch width. The

THIS
PAGE
IS
MISSING
IN
ORIGINAL
DOCUMENT

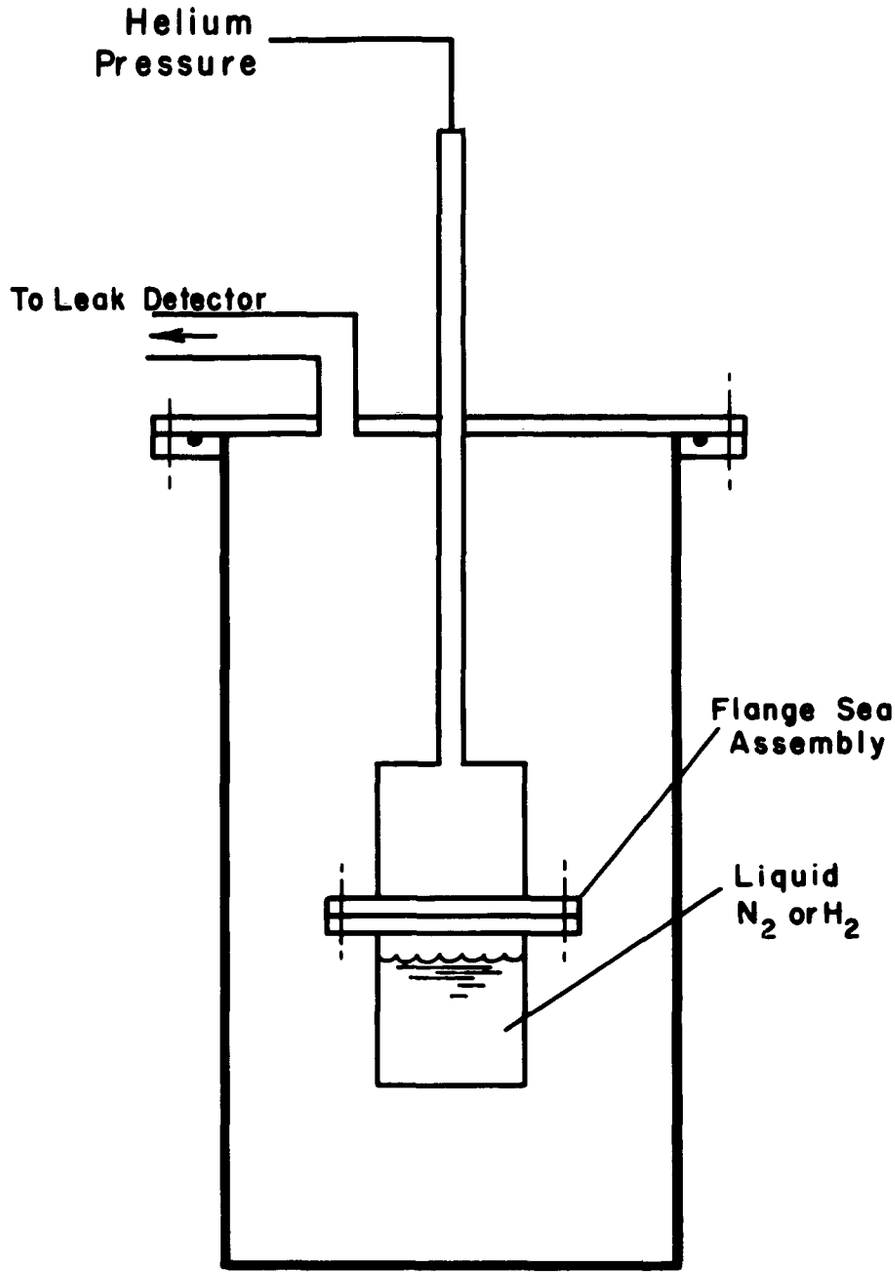

FIG. 3. Schematic of Seal Test Fixture

cycling was accomplished by means of an off-on switch which operated the three-port solenoid valve shown in Figure 3.

1.3.1 Extreme Lightweight Flange

One application involving airborne hardware required that weight be kept to an absolute minimum. The flange proposed for this application is shown in Figure 4. The flange, which fits a 3" O.D. pipe, was made of type 304 stainless steel with faces only .095" thick. There were eight holes for 1/4" bolts, equally spaced on a 4" bolt circle, and further reduction in weight was made by cutting out scallops of material between the bolt holes.

Various methods for sealing pairs of these flanges were tried, using three different seal materials. These were commercial o-rings of chlorosulfonated polyethylene and chloroprene and film of poly (ethylene terephthalate). On some of the o-ring tests a short stainless steel sleeve was fitted snugly inside the flange to hold the o-ring in position and prevent inward extrusion. A typical cross section of a flange assembly using such a sleeve is shown in Figure 5. Poly (ethylene terephthalate) film was used by making a "sandwich" of two flat gaskets separated by an o-ring shaped compression ring made of nichrome wire. The ends of the wire were tapered and silver soldered to make a smooth joint.

No really satisfactory method for sealing these extremely lightweight flanges was found. Some of the seals held at room temperature, and one o-ring used with the sleeve was leak detector tight at 76°K. But even this successful seal was probably borderline since a second attempt of the same kind failed when cooled to 76°K.

The reason for failure of these seals was lack of sufficient stiffness in the flange faces. Attempts to overcome this weakness by various schemes were not successful. It is felt that the flange could be designed for greater rigidity with little or no increase in weight. In the present design there is minimum stiffness between bolts, which is precisely where maximum stresses occur. The price of a more carefully engineered flange design is likely to be higher machining costs, but a rib between the bolt holes, for example, would not add much to the cost and would greatly improve the flange characteristics.

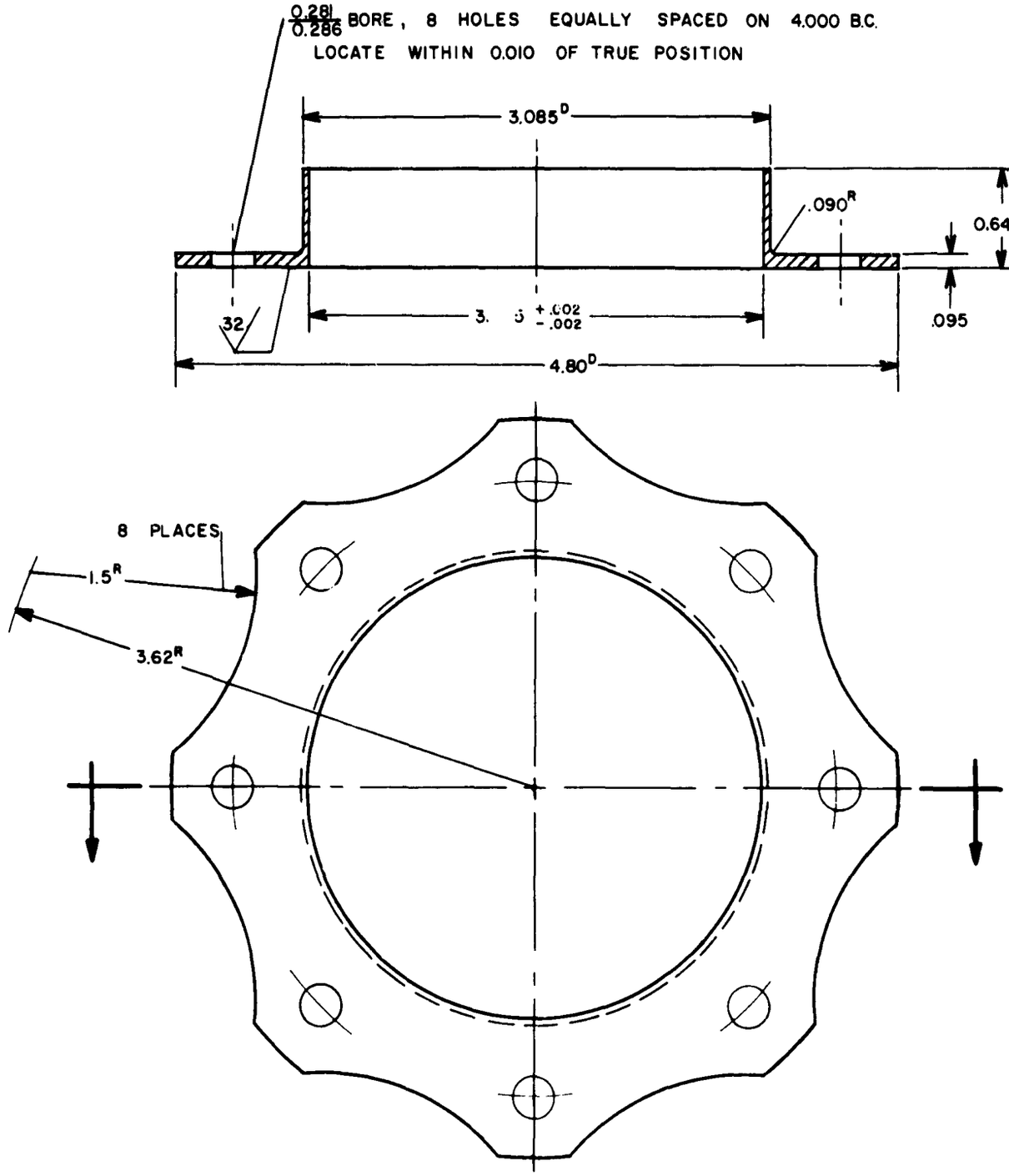

Scale: Full

Material: 304 S.S.

Note: Fractional tolerance ± 1/64

Decimal tolerance ± .010, except where noted.

FIG. 4. Extreme Lightweight Flange

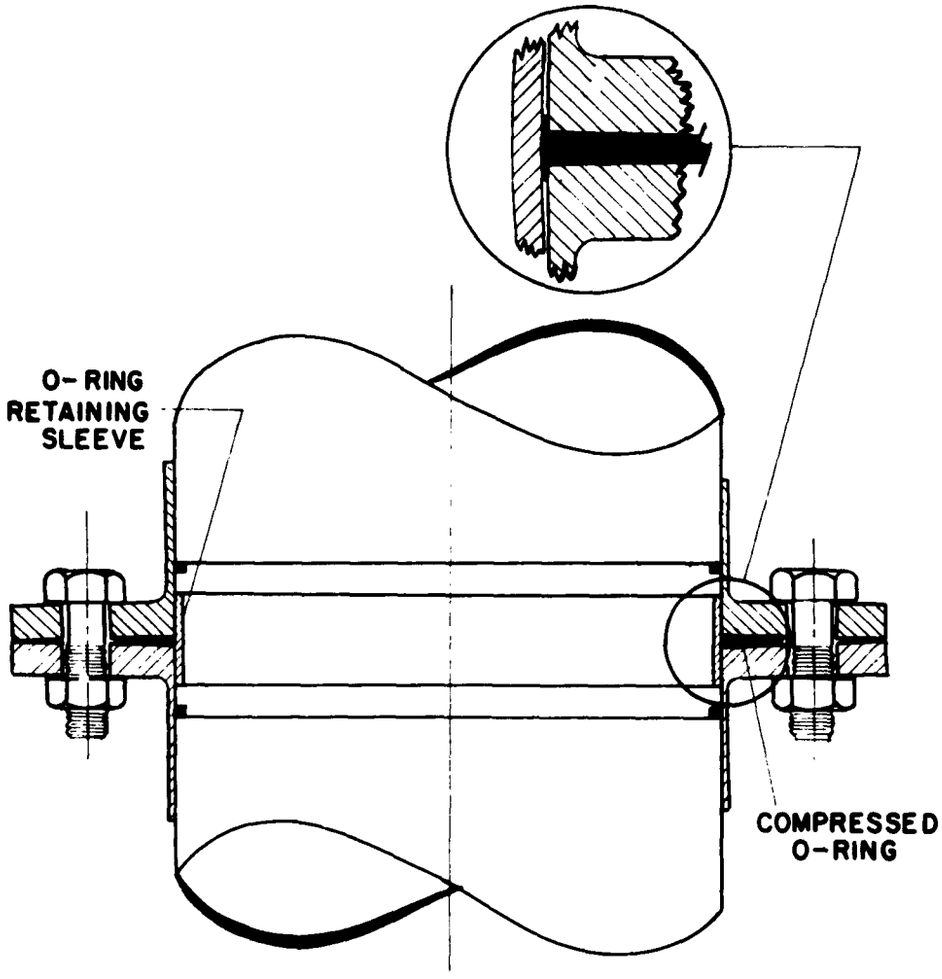

FIG. 5. Typical Flange Assembly with O-Ring Retaining Sleeve

1.3.2 Successful Flat Flanges

Additional flanges specified for the above program are shown in Figures 6 and 7. These flanges, for 2.5" and 3" O.D. pipelines respectively, were made of stainless steel with flange faces .200" thick. The smaller flange was drilled for ten 1/4" NF 18-8 stainless steel bolts on a 3.345" bolt circle, and the inside corner was given additional beef at the expense of some reduction in pipe I.D. The larger flange lacked this reinforced corner and used only 8 bolts (same bolts as the other flange) on a 4" bolt circle.

Certain parts of some fuel handling equipment call for a transition from stainless steel to aluminum. The flanges shown in Figures 6 and 7 were therefore duplicated from 6061, T6 aluminum, except that the flange faces were made .300" thick instead of .200". These were tested, both before and after anodizing to a black hardcoat finish, by mating with the corresponding stainless steel flanges. Except for the anodizing treatment, which was tested both polished and unpolished, all flange surfaces were used in the as-machined condition.

Table 4 gives the results of testing various combinations of these flanges with seals of readily available commercial o-rings and one film. The o-rings were compounds of chloroprene, chlorosulfonated polyethylene, and vinylidene fluoride/perfluoropropylene; the film was poly (ethylene terephthalate).

Successful seals were obtained with all of the flange combinations and with all of the seal materials. The film "sandwich" seal was very reliable when the proper combination of film thickness, compression ring cross section, and compressive force were used. In both types of seal a spacer ring to control the amount of compression would be advantageous. A machined step in one of the flange faces would also serve this purpose. The film seals require only about half as much flange loading as the .070-inch thick elastomer o-rings, but this advantage is somewhat offset by the fact that the elastomers can more easily adjust to flange irregularities. Another problem in the use of poly (ethylene terephthalate) film is the possibility of cracking if the compressive stress is too concentrated or too high.

An important factor present in these tests was flexibility of the flanges. In every case there was appreciable flexing of the flanges which resulted in a more or less uniform spring loading of the seals. In the case of the extreme lightweight flange, flexing was so non-uniform that a reliable seal could not be achieved. The other flanges flexed

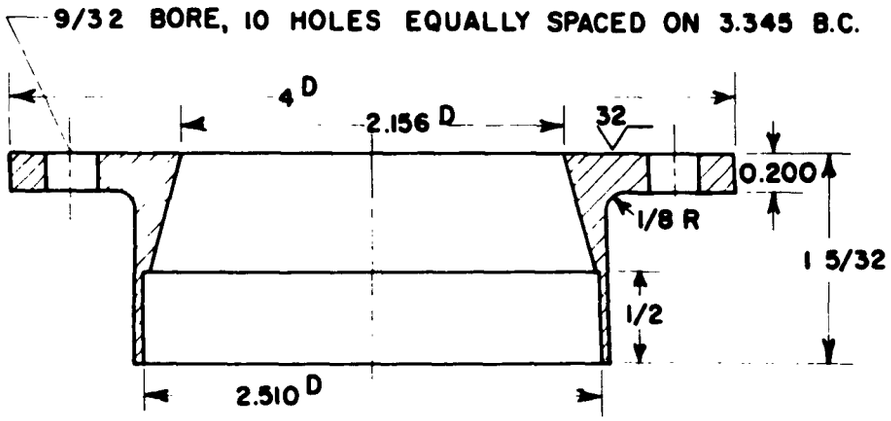

FIG. 6. Centaur Flange for 2.5 O.D. Line

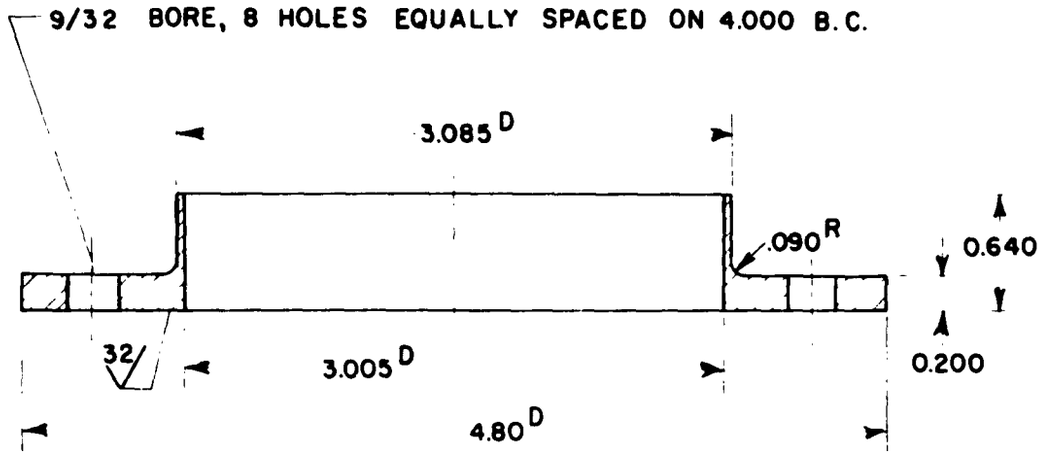

FIG. 7. Centaur Flange for 3" O.D. Line

Vinylidene Fluoride/Perfluoropropylene ("Parco" Compound 949-60)

Flange	O-Ring Size	Torque on Bolts	Comments and Results
Fig. 7 steel to Al.	2.864" I.D. .070"W	125 in-lb	Al. not anodized. Used retaining sleeve. No leak at 150 psig, room temp and 76°K.
ditto	ditto	ditto	ditto

Double Poly(ethylene terephthalate) with Nichrome Wire Between

Fig. 7 steel to steel	.0075" Film .065" Wire 3-1/4" Ring. Diam	100 in-lb	15 hot water to LN_2 cycles, 160°F overnight bake. 40 cycles, warm and cold, 150 psig to 1 atm. No leak at 250 psig room temp. No leak at 150 psig 76°K.
Fig. 7 steel to steel	.0075" Film .065" Wire 3-1/4" Ring. Diam	75 in-lb	ditto above except no 160°F bake. No leaks warm or 76°K. 80 pressure cycles.
ditto	ditto	60 in-lb	Slight leak both warm and 76°K at 150 psig.
ditto	ditto	70 in-lb	No leak warm and 76°K at 150 psig. Leaked cold at 240 psig.
ditto	.005" Film .065" Wire 3-1/4" Ring Diam	75 in-lb	Leaked warm. Film cracked when increasing torque.
Fig. 7 steel to steel	.0075" Film .050" Wire 3-3/16" Ring Diam.	100 in-lb	OK warm, leaked cold. Warmed and torqued to 125 in-lb, which cut through the film.
Fig. 7 steel to Al	.0075" Film .050" Wire 2-11/32" Ring Diam.	75 in-lb	Leaked warm. Torqued to 80 in-lb, which cut through the film.

Table 4. SEAL TESTS USING 2.5" and 3" DIAMETER FLAT FLANGES

Flange	O-Ring Size	Torque on Bolts	Comments and Results
		Chloroprene ("Parco" Compound 307-50)	
Fig. 7 steel to steel	3.239" I. D. .070" W	75 in-lb	Flange edges just touched. OK warm. Leaked while cooling.
ditto	ditto	180 in-lb	Additional squeeze after flange edges touched. Seal deformed inward to flower shape. Leaked warm.
ditto	ditto	120 in-lb	OK warm. Leaked approx. 1 liter/ hr when cold.
Fig. 6 steel to Al.	2.614" I. D. .070" W	125 in-lb	Al. anodized, unpolished. Temp cycled twice, pressure cycled to 160 psig 5 times. No leak at 76°K.
ditto	ditto	ditto	Al. anodized, polished. No leak at 76°K, 160 psig.
		Chlorosulfonated Polyethylene ("Parco" Compound 921-50)	
Fig. 7 steel to steel	3.489" I. D. .070" W	155 in-lb (Flange edges touch at 50 in-lb)	Pressure cycled 1 atm to 160 psig 40 times during cooldown, 25 times at 76°K. Temp cycled 25 times. No leak.
ditto	3.350" I. D. .070"W	100 in-lb (Flange edges touch at 50 in-lb)	OK warm, held 1 atm at 76°K Small leak at 150 psig, 76°K
Fig. 6 steel to Al	2.614" I. D. .070" W	135 in-lb	Al. not anodized. OK warm. No leak at 76°K, 240 psig: No leak at 20°K, 150 psig.
Fig. 7 steel to Al	2.864" I. D. .070" W	125 in-lb	Al. not anodized. Used sleeve. OK at 150 psig warm. Leaked during cooldown.
ditto	ditto	150 in-lb	Same as above except torque No leak warm or 76°K
ditto	ditto	ditto	Newly machined steel flange. Used sleeve No leak warm or 76°K, 225 psig.
Fig. 7 steel to Al	3.239" I. D. .070" W	150 in-lb	Al. not anodized. Temp cycled 5 times, pressure cycled 10 times. No leak at 76°K, 150 psig.
ditto	ditto	ditto	Al. not anodized. Used retaining sleeve. No leak at 150 psig and room temp, 76°K, 20°K.

Table 4 (Continued) SEAL TESTS USING 2.5" and 3" DIAMETER FLAT FLANGES

into a fairly uniform cone shape (although some of the seals deformed into a flower pattern, showing some bowing between bolts). When the flexing was relatively uniform it served to reduce the initial compression required to maintain the seal during cooldown. Measurements indicated that good seals were being made with 65 to 70% compression of the o-ring, whereas 80 to 90% is required if spring loading through distortion of flange parts is eliminated.

2. Moving Seals

An apparatus for study of packings for slow-turning shafts has gone through several modifications and is shown in its present form in Figure 8. It was necessary to go to the double seal arrangement shown in order to eliminate end thrust on the shaft when pressure was applied to the seal. Attempts to oppose this thrust through a ball bearing were partially successful, but measurements of the torque required to turn the shaft were more difficult to interpret because the resistance of this bearing varied with pressure and temperature. Another important improvement in the present apparatus is lining the packing sleeves with molybdenum-filled and reinforced polytetrafluoroethylene.

The shaft is turned at 16 rpm through a variable clutch and flexible drive. These allow the tests to be performed with the jig clamped in a vice on the bench or, alternately, in a dewar of liquid nitrogen or hydrogen. Preliminary tests with chevron-type packings of polytetrafluoroethylene indicate that the problem of bearing resistances has been solved. The apparatus is presently on a stand-by basis with no testing planned for the immediate future.

Figure 9 is a sketch of a high speed rotating seal tester which has been designed for testing bellows-type face seals. There is an important need for work in this area, and considerable effort has gone into the background and test design study. Much of the equipment and instrumentation for the tester shown in Figure 9 is on hand, but the program has been halted short of machining and assembly stages because of budget limitations.

3. Physical Properties Program

3.1 Properties and Their Relation to Sealability

3.1.1 Compression Dilatometer

When an amorphous rubber-like material composed of long chain molecules randomly distributed is compressed, the chains tend

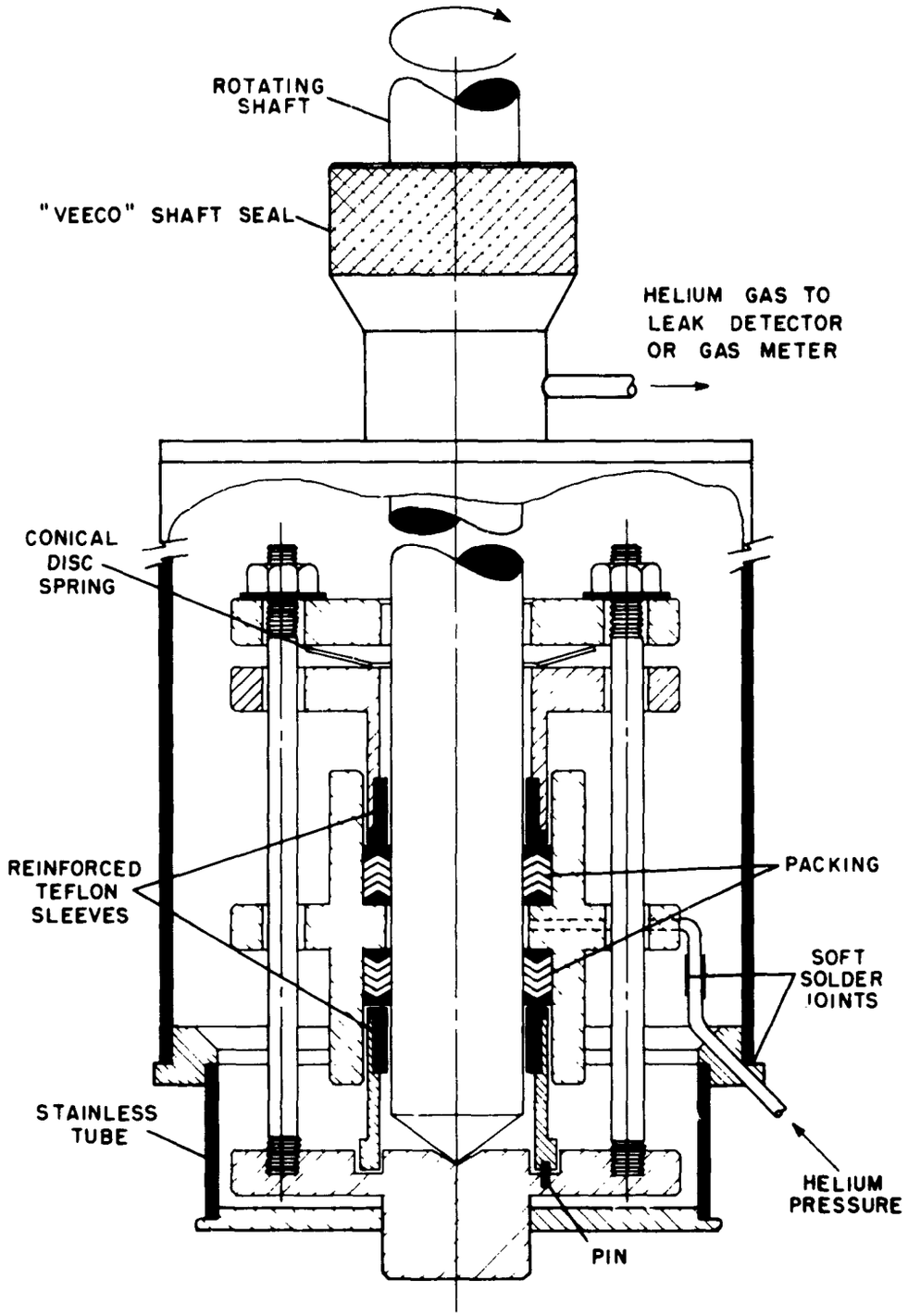

FIG. 8. Packing Tester for Low-Speed Rotating Shaft

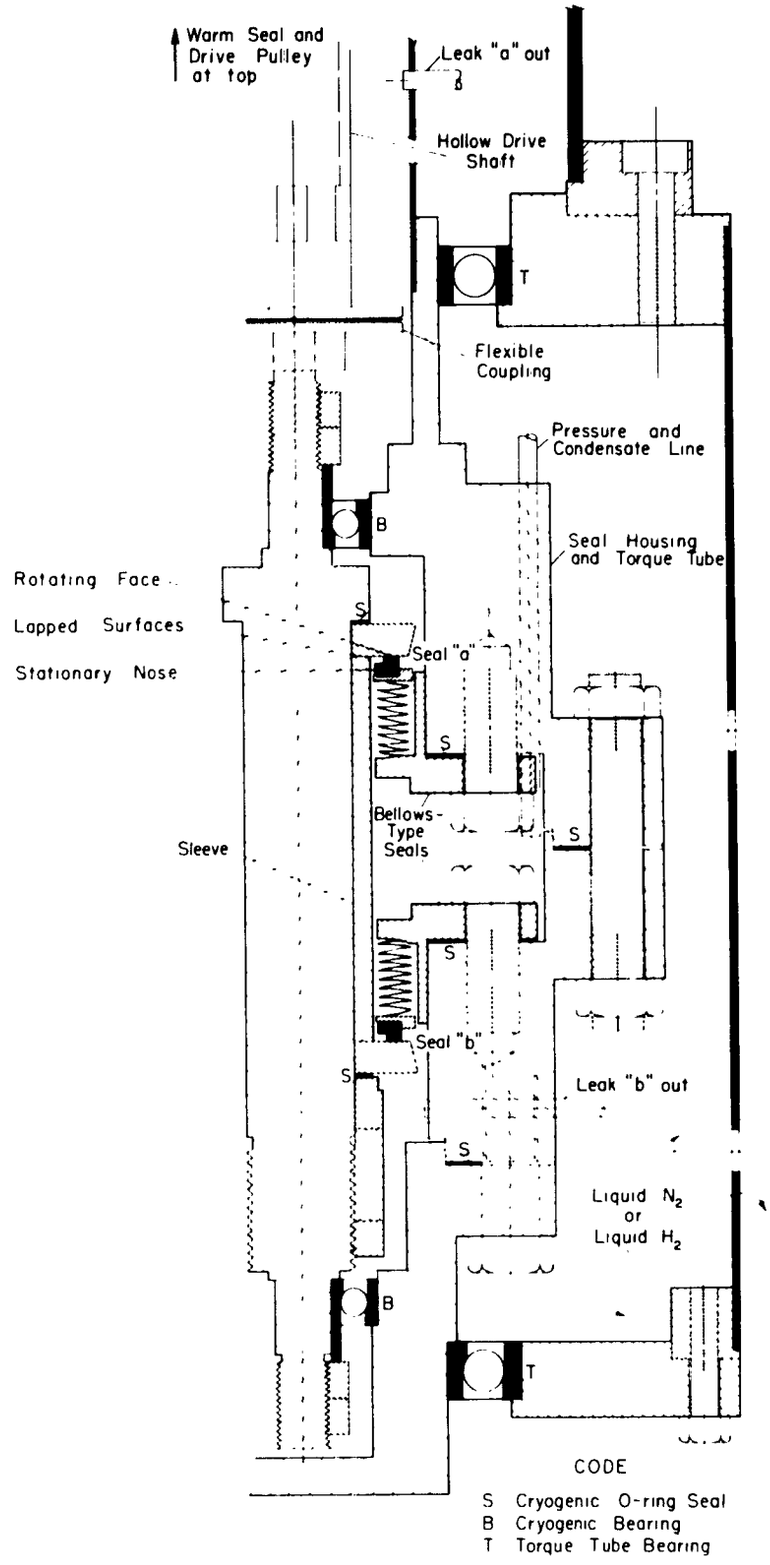

FIG. 9. High Speed Rotating Seal Tester

to become more oriented. For most copolymers and polymers with complex side chain constituents this orientation does not lead to crystallization, but it does result in anisotropy. To investigate the behavior of elastomers compressed highly and subsequently cooled to some low temperature, the apparatus shown in Figure 10 was designed and built. Specifically, the contractions of 1/2-in thick by 1 in^2 cross section compression set buttons when compressed 20-50% and cooled to 76°K, were studied. To measure contraction for a wide range of initial applied forces, a bellows capable of translating 3000 lbs. force to the sample was obtained. The actual bellows pressure used varied from 20 psi to 500 psi, and was kept constant for the duration of each test. Length measurements were made by using a lever which translated vertical movement of the sample and part of the stainless steel compression platens into horizontal movement outside the cold area. Several compression platens were used, each having a different length; accordingly, the same lever could be used for widely varying values of initial contraction. Contraction of the long vertical portion of the stainless steel lever had a very small effect on the measurements, but calibration of the lever was necessary due to contraction between the fulcrum and the lever pointers touching the top compression platen. The bellows top plate was free to move with the sample and was aligned by three rods connecting the stationary brass plates. Two thermocouples were attached to the sample just before cooldown, and temperatures were recorded continuously during the tests. The dilatometer was cooled by continuously transferring cold nitrogen (gas initially, and liquid during final cooldown) into the dewar which surrounded the dilatometer. Since large masses of brass and stainless steel were in contact with the sample, no further means was provided to insure uniform cooling. Cooling rate was controlled by regulating the pressure over the supply dewar, and rates as low as 0.5 K°/min were attained in this manner.

This apparatus was developed to measure contraction of compressed elastomers during cooldown. Before preliminary results are presented, a brief discussion of what causes the contraction is in order. Even before the sample is cooled, a time-dependent deformation begins: as time increases, the sample contracts. Other investigators have shown deformations at around 300°K, due to shear strain, to be a linear function of log time in the range one minute to one week[2], and the same dependence is expected in compression.

As the elastomer starts to cool, creep continues at a somewhat reduced rate, and at least two other effects add to the overall contraction. First, the normal volume contraction causes linear shrinkage; it is

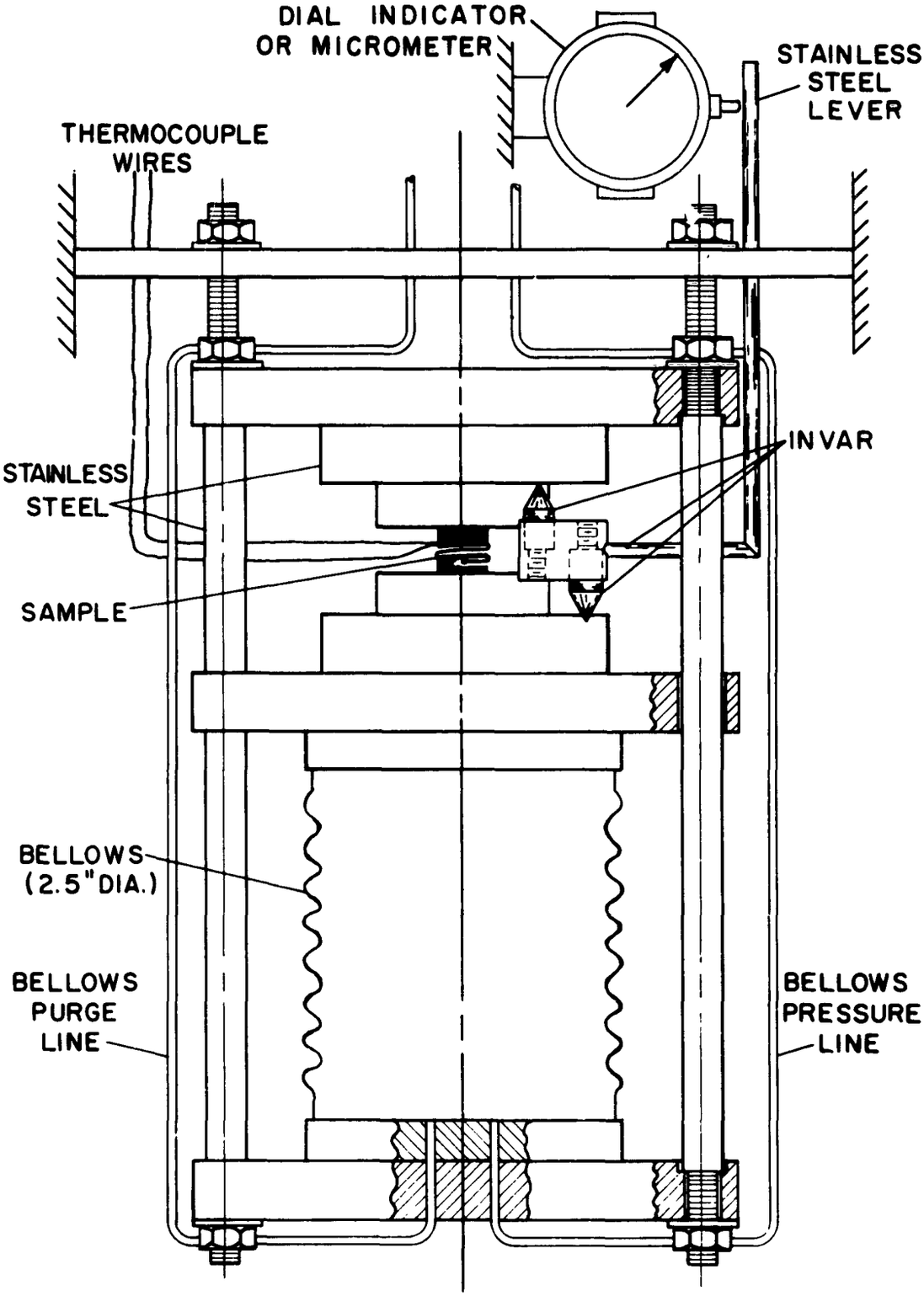

Fig. 10. Compression Dilatometer.

expected that the amount of this contraction is changed by the configurational changes in the compressed sample, but experimental verification has not been possible. Secondly, an appreciable linear contraction at constant volume is caused by the applied force when the sample is cooled. This effect, due to molecular configuration considerations, is referred to as the Gouge-Joule effect by Payne and Scott[3] and predominates at temperatures above the glassy-state transition.

The above effects change radically when the elastomer reaches its glassy-state transition temperature. At this point, random thermal motion of the chains is inhibited by the fact that free rotation of chain elements about single bonds will not take place at an appreciable rate, and the material becomes hard and rigid like a glass. At temperatures below this point (T_g) the behavior is similar to that of any ordinary solid. Therefore the Gough-Joule effect, as well as the creep effect, does not appear below T_g. Only the normal thermal expansion below the brittle point should be present.

The results shown in Figures 11 and 12 were obtained using commercially available samples of a copolymer of hexafluoropropylene and vinylidene fluoride. It should be emphasized that the results are still preliminary in nature, and thus should be considered qualitative rather than quantitative. Figure 11 is a plot of the contraction of a 1 in^2 x 1/2 in elastomeric button as a function of time. This sample was compressed 24%, corresponding to a pressure of 150 psig. Before cooldown the contraction was a linear function of log time, which agrees with the results in shear as previously mentioned. After cooldown had begun, the normal thermal contraction and Gough-Joule effect added to the already rapid contraction until the glassy-state transition was complete, after which only a small change in length was observed, not discernible on the scale used in this plot.

Figure 12 shows how the overall contraction of the material can be reduced by keeping a small strain on the sample for several days. During the pre-stressing period at room temperature the stress was about 40 psi, and resulted in an appreciable reduction in contraction during cooldown. It is believed that this small stress could not have induced crystallinity, or otherwise affected the true properties of the elastomer[4]. The reduction is attributed solely to diminishing the contribution of creep. The obvious conclusion is that if an o-ring were stressed prior to actual use (by assembling the seal ahead of time, for example) and then re-stressed just before using (by re-tightening the bolts) it would effect a satisfactory seal at lower

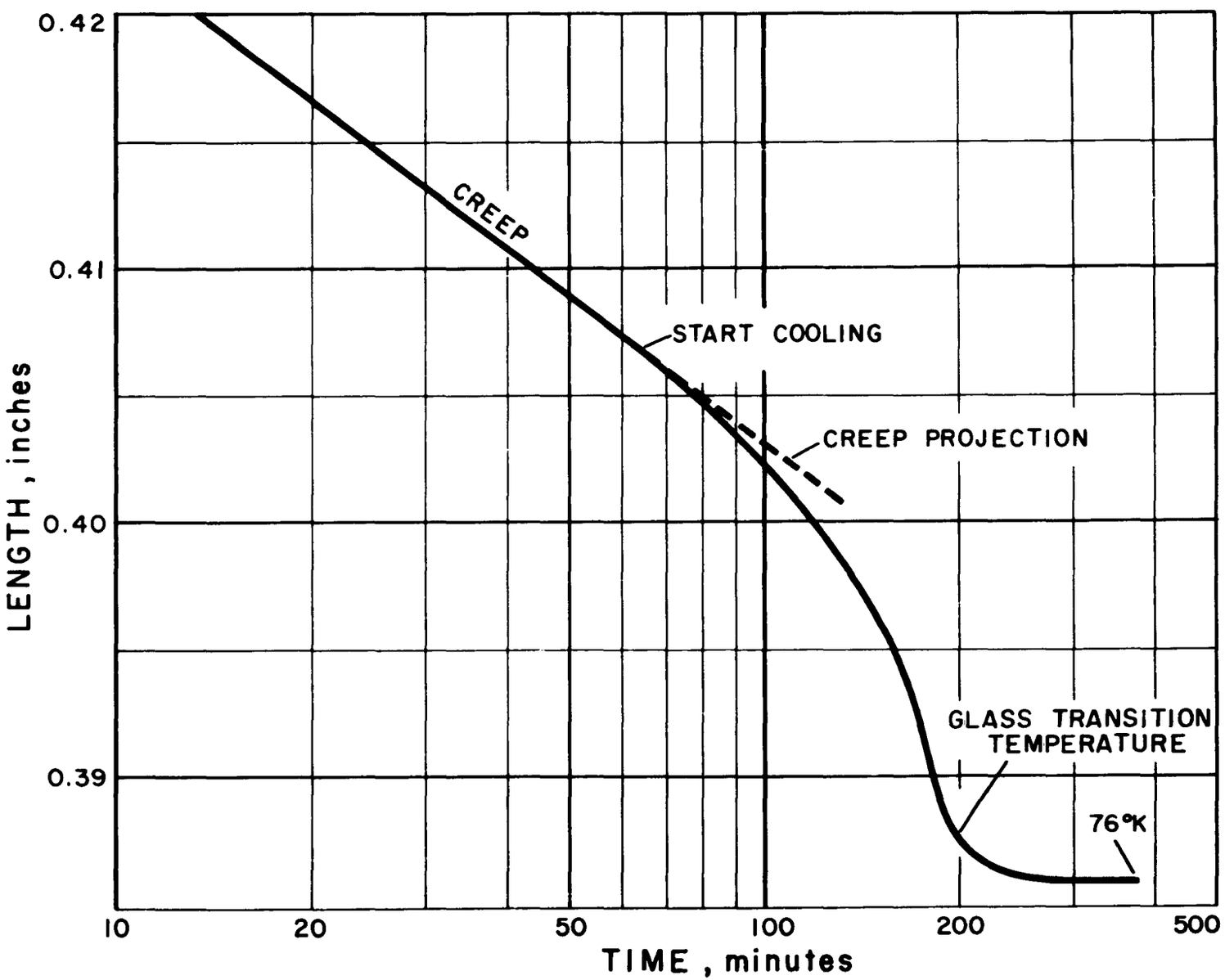

FIG. 11. Contraction of Compressed Elastomer Before and During Cooldown

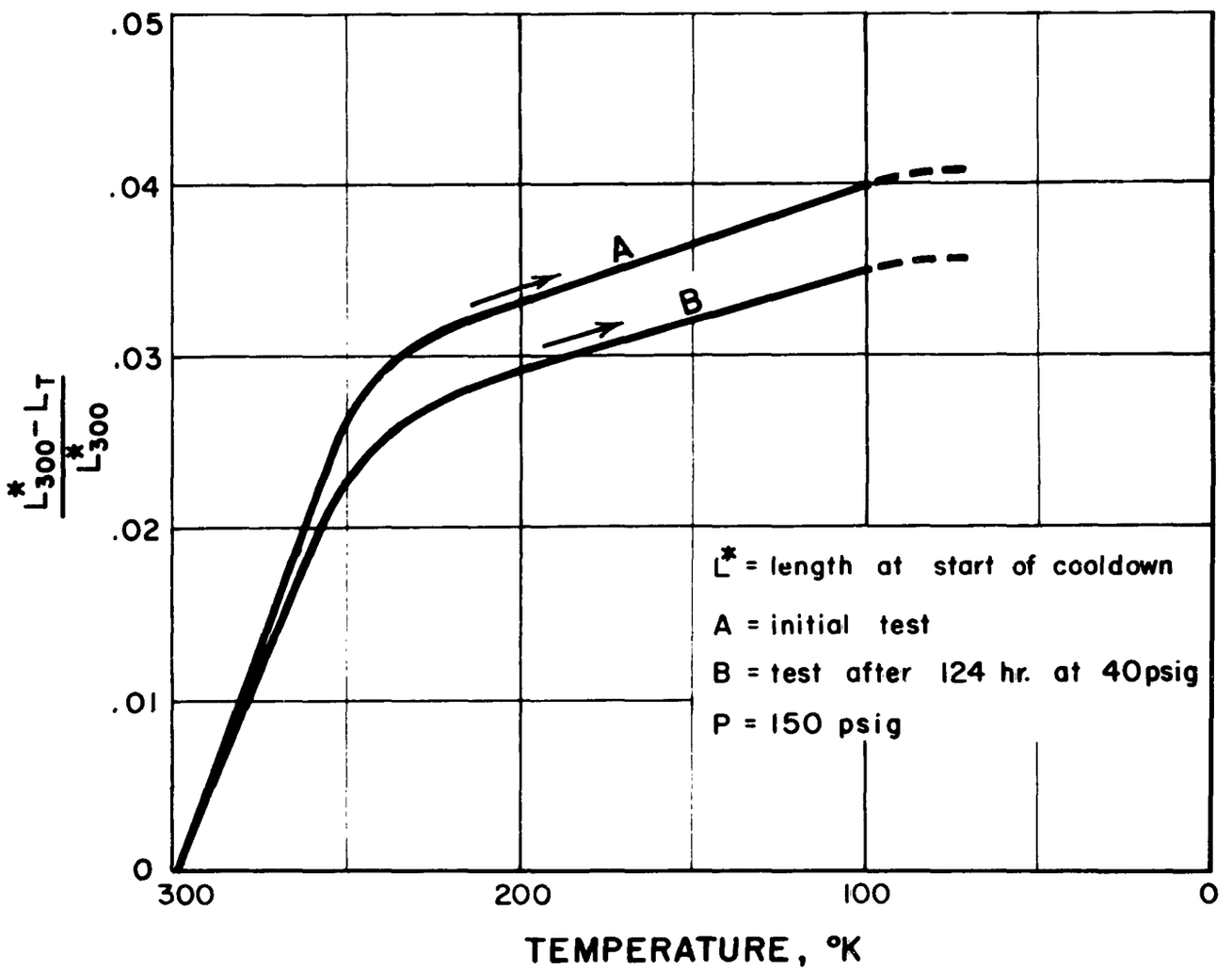

FIG. 12. Thermal Expansion Before and after Sustained Strain

temperatures than if the pre-stressing were not performed. Alternately, a smaller squeeze (and smaller bolt torque) would effect a good seal at some given temperature. This result was observed in a few of the functional seal tests, but has not been studied with specific reference to creep effects.

3.1.2 Sealing Theory

We suggest now a method for analytically treating the system where an o-ring is compressed between two flat plates and cooled for sealing service in the cryogenic temperature range.

When an o-ring is compressed by bolts between two metallic flanges, the effectiveness of the resulting seal depends solely on the existence of a force normal to the surfaces of the flange faces. During cooldown this force must remain above a minimum value determined by the system pressure required in the specific application. To determine how the force varies with temperature the following analysis is offered to relate experimental measurements with sealability.

Considering only the changes in force on the sample due to temperature change, the relation between the stress (σ_{T_1}) at T_1 (initial) and that at T_2 is [5]

$$\sigma_{T_1} - \sigma_{T_2} = \alpha E(T_1 - T_2) \tag{1}$$

The coefficient of expansion α, and E, the modulus of elasticity in compression, are assumed constant. If α and E vary, their product must be integrated over the temperature range in question, giving

$$\sigma_{T_1} - \sigma_{T_2} = \int_{T_1}^{T_2} \alpha E \, dT \tag{2}$$

for the change in force with temperature after pre-loading at T_1. In the actual situation, length changes due to bolt and flange shrinkage during cooldown also affect the stress, and they may be taken into consideration in the following way. Since all force changes are a function of either temperature or sample length, L, we may write

$$\sigma = \sigma(T, L)$$

which, upon differentiation, gives

$$d\sigma = \left(\frac{\partial \sigma}{\partial T}\right)_L dT + \left(\frac{\partial \sigma}{\partial L}\right)_T dL \qquad (3)$$

A common identity gives us

$$\left(\frac{\partial \sigma}{\partial T}\right)_L = - \left(\frac{\partial \sigma}{\partial L}\right)_T \left(\frac{\partial L}{\partial T}\right)_\sigma \qquad (4)$$

Multiply the right side of equation (4) by L/L:

$$\left(\frac{\partial \sigma}{\partial T}\right)_L = L\left(\frac{\partial \sigma}{\partial L}\right)_T \frac{1}{L}\left(\frac{\partial L}{\partial T}\right)_\sigma$$

By definition:

$$L\left(\frac{\partial \sigma}{\partial L}\right)_T = E, \text{ and } \frac{1}{L}\left(\frac{\partial L}{\partial T}\right)_\sigma = \alpha$$

Substituting in (3) gives

$$d\sigma = -\alpha E dT \frac{E}{L} dL \qquad (5)$$

The first term is identical with that given in equation 1, and the second term takes into consideration all length changes from "external" sources, such as bolt shrinkage. Integrating (5) we get:

$$\sigma_2 = \sigma_1 \int_{L_1}^{L_2} \frac{E}{L} dL - \int_{T_1}^{T_2} \alpha E dT. \qquad (6)$$

dL is a function of T also, due to shrinkage in the bolts and flanges, so the temperature function could be used to evaluate this integral. If only α and T affect the stress, equation (5) shows that, if volume changes and end effects are small, the stress at any temperature T_2 may be estimated by knowledge of: 1) the initial stress; 2) continuous curves of E vs T and α vs T for the sample; and 3) the bolt shrinkage. However, if the flanges have flexed during the room temperature preload, changes in the flex angle will help maintain σ. Consequently, less initial stress is needed to achieve a required stress at some low temperature if flange flexing is present.

3.2 Force Evaluation Experiment

The purpose of this experiment is to measure the variation in the force exerted by a compressed o-ring as the o-ring is cooled from 300°K, through the brittle transition point to 76°K.

The apparatus employed is shown in Fig. 13. This is essentially the heavy flange o-ring tester shown in Fig. 2 on page 5, modified to contain an assembly of washer-type force gages which measure the force on the o-ring. Previous experiments have proven it absolutely necessary to maintain the force gages at a constant temperature. This is accomplished by immersing the whole gage assembly in liquid nitrogen, which is contained by a sealed flexible bellows.

The force washer assembly contains three washers (only one is shown in Figure 13) which are strained and one temperature compensating washer which is not strained. The strained washers have loading sleeves on each side which serve to minimize friction as increased loading tends to slightly extrude the force washer and stretch the resistance wire wrapped around it. By using the three strained force washers as one arm of a Wheatstone bridge, and the unstrained washer as a second arm, the ΔR resulting from force on the strain sensitive wire will show a bridge imbalance. This imbalance is calibrated in terms of force exerted on the washers.

Four thin layers of mica insulation are placed on the top and bottom of the bellows caps to provide insulation for the bellows assembly. The floating plate further isolates the o-ring from the liquid nitrogen in the bellows and transmits the force exerted by the o-ring.

Thermocouples are placed at the points indicated to check the average temperature of the o-ring, the ΔT across the o-ring, and the temperature at the middle of the stud.

Initially, the o-ring is compressed to some arbitrary value (usually 70%) by tightening the stud nuts. This gives a definite initial loading force. At the start of cooldown the whole apparatus is immersed in liquid nitrogen. Cooling starts from the entire exterior surface. Nitrogen also flows through the stainless steel tube into the bellows and starts cooling from the inside.

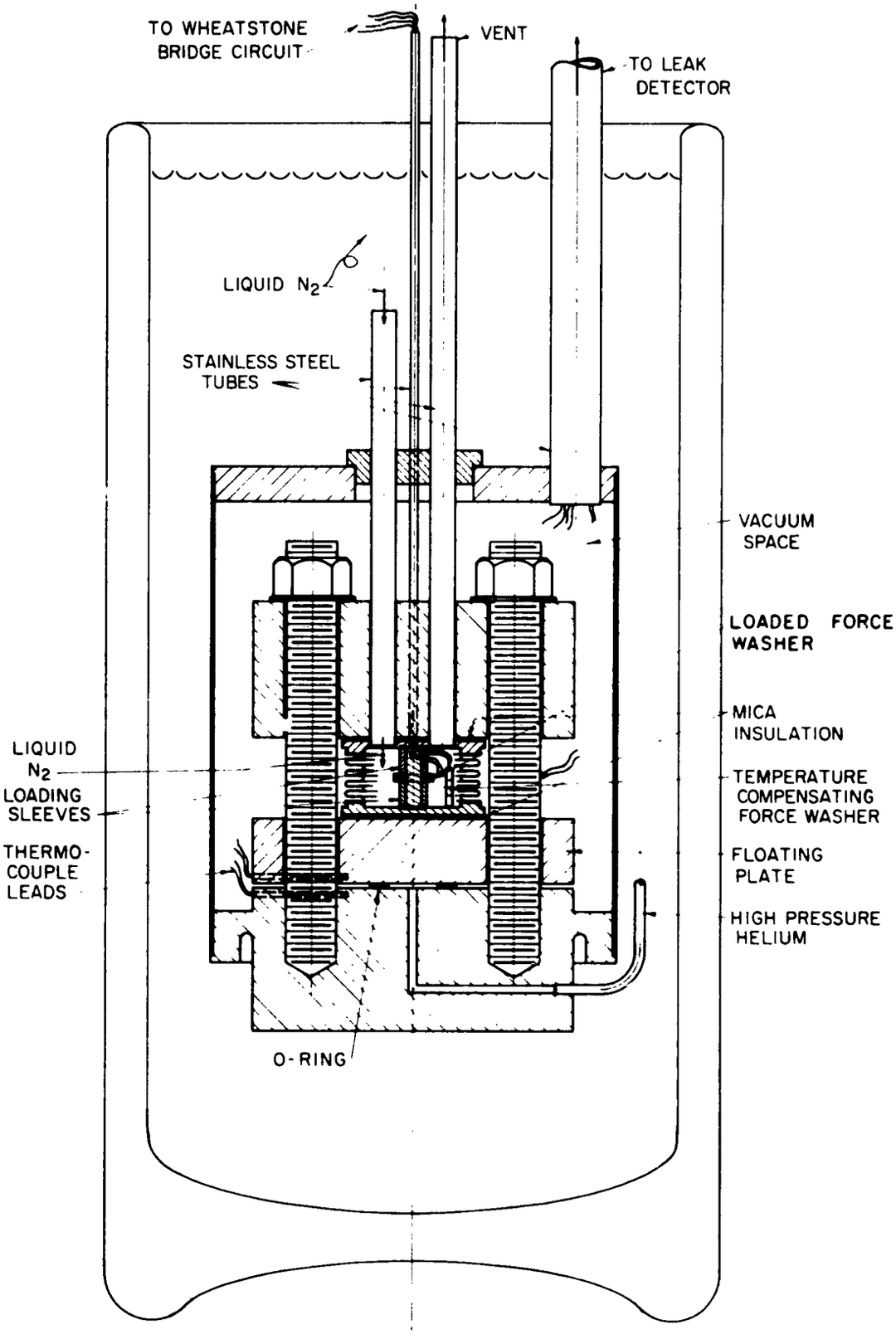

FIG. 13. Force Evaluation Test Jig

Ideally, the thickness of the compressed o-ring should remain constant during cooldown and any variation in force shown by the washers would be due to the thermal contraction of the o-ring. Actually, this ideal condition does not exist because of differential contraction between the studs and strain gage assembly.

The differential contraction takes place in the following manner. The force washers, loading sleeves, and bellows caps come to liquid nitrogen temperature as soon as liquid nitrogen enters the bellows. The total contraction of these components is approximately .004". This lowers the initial compression and decreases the initial force on the o-ring. As the cooldown continues, the six studs begin to contract slowly. This much slower cooldown and contraction of the studs gradually restores the initial loading force.

The results of this differential contraction are easily seen in Fig. 14. For one cooldown a stainless steel disc was used instead of an elastomer o-ring. During the first four minutes the force decreases approximately 8600 lbs., then gradually increases back to the initial loading force as the studs contract.

For comparison, there is a similar curve for which an ASD neoprene o-ring was used. Again the initial unloading is present, but it is less because of the elasticity of the rubber as compared to the stainless steel disc. The gradual increase in force, as the stud temperature drops, is again present. The bottom part of this curve is not reproducible, which is attributed to the differential contraction problem and not to the change in force brought about by the cooling o-ring. It has become evident that the differential contraction problem must be eliminated or made negligible if the force variation of a cooling elastomer o-ring is to be measurable.

At present a modification is under way which should almost eliminate the differential contraction problem. This modification eliminates the floating plate and places the insulated bellows arrangement directly on top of the elastomer o-ring. The loading sleeves will be made of invar instead of stainless steel. In addition, a 3/4-inch diameter invar pillar will be placed adjacent to each stud. These pillars will be very securely tightened between the 2" thick top plate and the 2" thick base. Invar is being used because its thermal expansivity is only 10% that of stainless steel throughout the temperature range of interest.

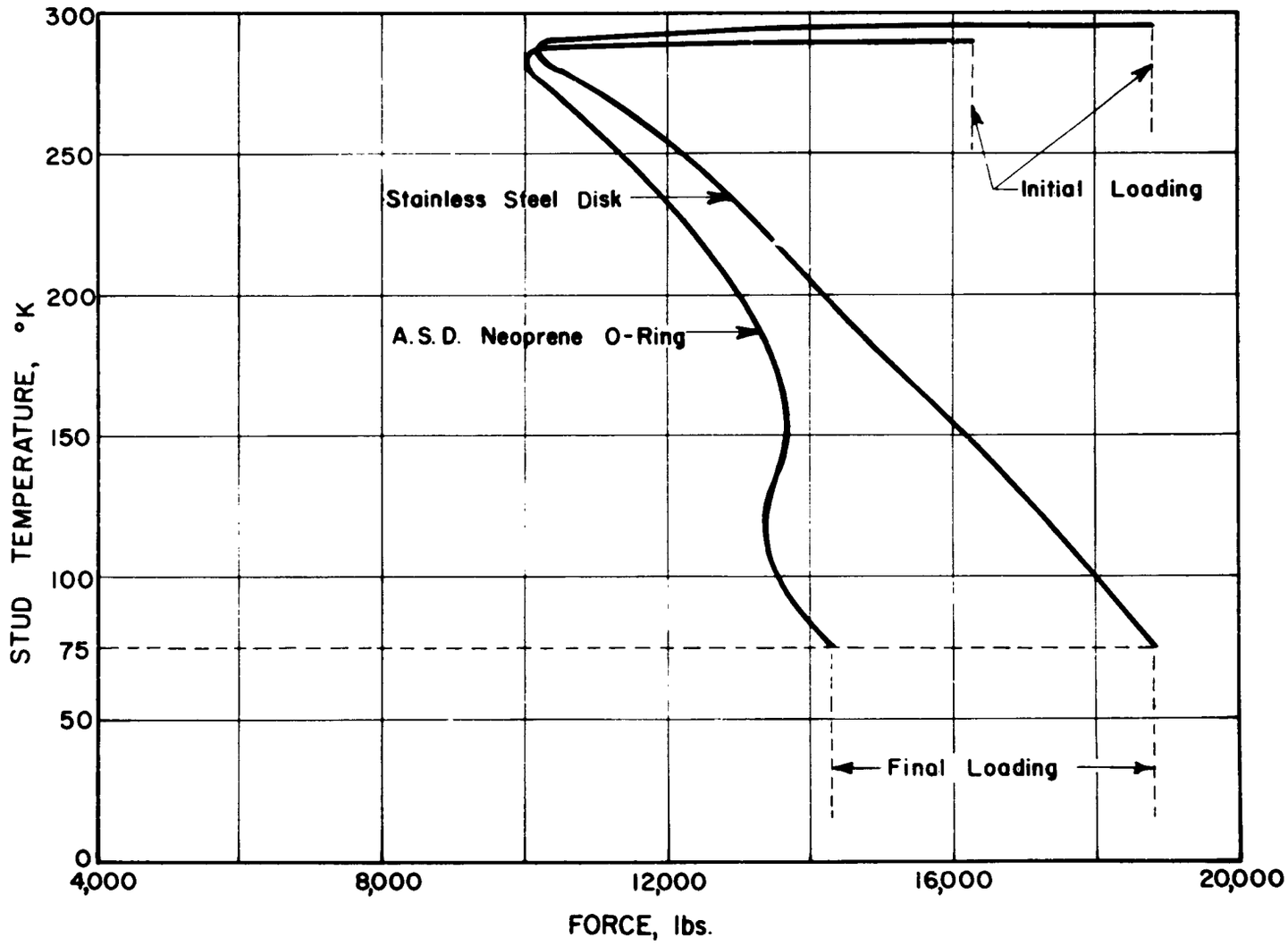

FIG. 14. Forces During Cooldown

With this arrangement there will be an initial contraction of the invar sleeves, force washers, and bellows caps. This will take place immediately and the "initial" force on the o-ring will be taken at this point. After this initial contraction, the only further contraction affecting the percent of compression will be due to the invar pillars contracting; this should be about .0004" instead of .008" as with the previous arrangement.

3.3 Thermal Expansion and Second Order Transitions of Polymers in the Temperature Range 300--76°K

3.3.1 Introduction

In the reporting year considerable effort has been directed toward the experimental measurement and theoretical understanding of the second order transition point (T_g) and the thermal expansion of polymer materials classed as elastomers. The objectives of this part of the program are three-fold:

1. To experimentally measure the low temperature thermal expansion of elastomers, most of which have not been reported comprehensively in the literature. Thermal expansion can be related to o-ring sealability, and is important in other possible low temperature uses of elastomers.
2. To relate the thermal expansion to molecular structure and compounding procedures, with the idea of directing the synthesis of materials with lower thermal expansions.
3. To determine the direction to be taken if one tried to synthesize a gum elastomer of appreciably lower T_g than those available at present.

A dilatometer has been developed to measure thermal expansions at low temperatures, and some measurements have been made. The results, together with a brief discussion of thermal expansion and some possible interpretations of the measurements, will be reported.

3.3.2 Brief Theory

Thermal expansion of polymers seems to be due to changes in the configuration of the chains. The expansion is due not so much to the motion of one chain past another, but to the internal motion of the units within the molecules[6]. This change depends on the energy changes of the long chain molecules and the units which make up the molecules, and on the various forces present. These forces include surface tension, primary atomic forces, and secondary molecular forces. The forces can be varied by many methods: 1) inserting fillers, 2) plasticizing, 3) varying molecular weight (length of chain), polarity, symmetry, and orientation.

The two commonly designated points which signify the stiffening of an elastomer when it is cooled are T_g and the brittle point. The T_g of high polymers is usually very close to the brittle point. The T_g is the temperature at which the rotation of the units in the molecules of polymers stops or begins, depending on whether one is following the temperature up or down. The brittle point is the temperature at which a substance shatters under specified standard test conditions. This depends on how fast the molecules can absorb the applied force. If the molecules do not react fast enough, the material shatters.

The T_g arrived at experimentally by thermal expansion tests and the thermal expansion coefficient itself are dependent slightly on the rate of temperature change. Ideally, the sample should be allowed to come to equilibrium at infinitesimal successive ΔT's. In this case, the total thermal motion of the molecules would be accounted for. In the real case, some of the thermal expansion action is "frozen" before it is completed. For example, when contracting, the molecules have a smaller effective volume, creating "holes", which gradually diffuse to the surface. Some of these "holes" are frozen inside the sample. But since the amount of contraction which takes place below T_g is small compared to the overall contraction usually measured, this effect is small. However, if the rate is very great, as in quenching, the effect can be noticeable[7].

3.3.3 Apparatus and Procedure

Figure 15 shows the dilatometer which is being used to measure thermal contraction and expansion of elastomer samples in the temperature range of 76 to 300°K.

A 2-inch long by 1/2-inch diameter sample is surrounded by a heavy-wall copper tube or shield which helps maintain uniform sample temperature. The sample and tube are supported by three invar rods connected to a brass top plate. On top of the sample rests an invar rod with brass ends, which applies a constant force of 98 grams to the sample. The top plate and sample support assembly can be easily lifted out of the cooling system in order to change samples.

Around the sample support assembly is a second copper shield which has soldered around it a coil of copper tubing which carries a small flow of nitrogen gas. This gas is discharged inside the shield, near the bottom, and serves as the heat transfer medium which cools the sample. The shield is supported and surrounded by expanded polystyrene which serves as insulation to slow down the cooling rate.

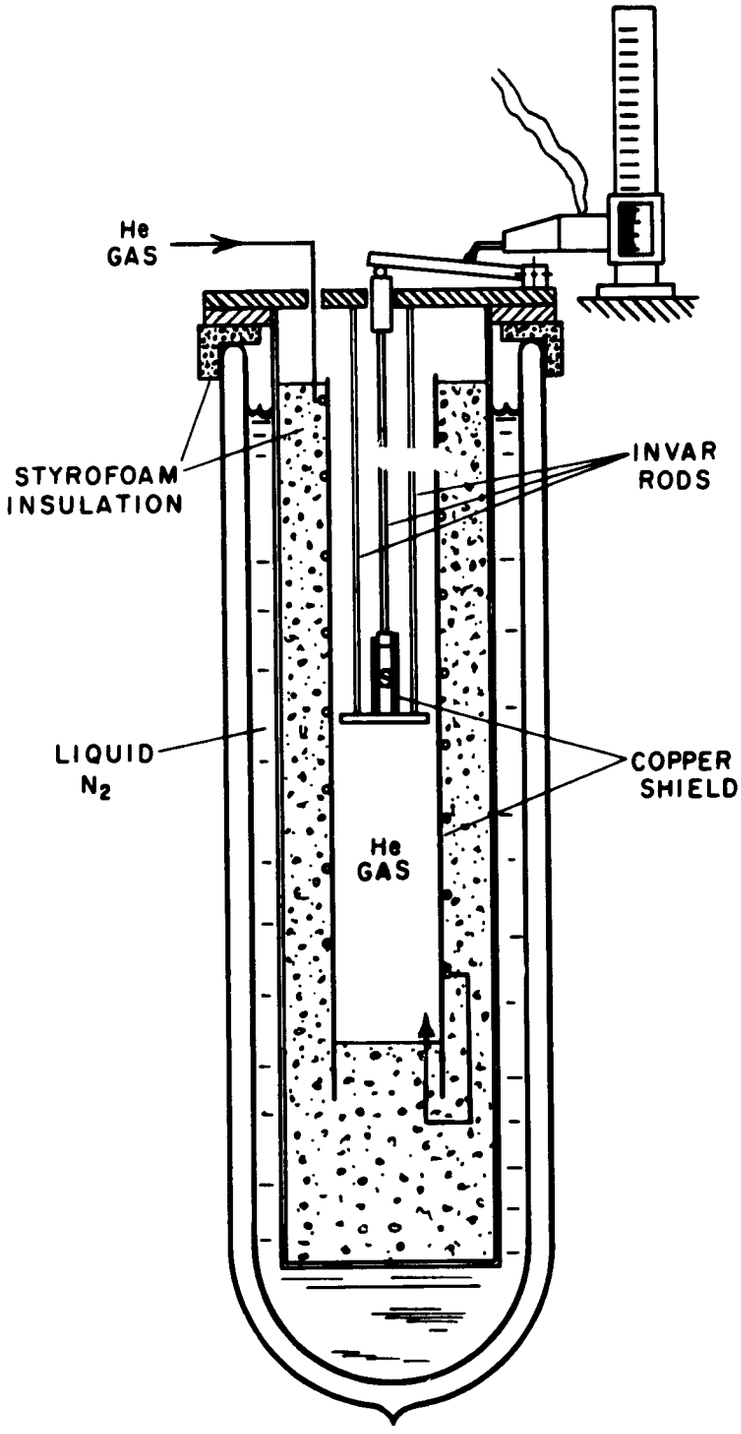

FIG. 15. Cryogenic Dilatometer

The polystyrene is enclosed by a flanged metal can which is immersed in a bath of liquid nitrogen. Thus the major part of the cooldown is by slow conduction through the N_2 gas and expanded polystyrene surrounding the sample. The final part of the cooldown is achieved by introducing liquid nitrogen directly into the space around the sample. Average cooldown rate is maintained at about 40 Kelvin degrees per hour.

Both length and temperature are measured electrically, and continuously recorded by a 6-point millivolt recorder. One thermocouple (introduced with the aid of a sewing needle) is located inside the sample and a second thermocouple is taped to the sample surface. When these temperatures are not exactly the same, an average of the two is used. Length measurement is achieved by means of a sensitive differential transformer which is activated by a hinged finger. The free end of the finger rests on a lever which moves up and down as the length of the sample changes with temperature. Sensitivity can be adjusted by moving the transformer to different positions along the length of the lever. Calibration is achieved at constant temperature by slipping the leaves of a thickness gauge between the lever and the top of the rod which rests on the sample. A check on the accuracy of the entire system was made by using a sample of pure aluminum having known expansivity. Overall accuracy is about ± 3%.

3.3.4 Results and Interpretations

To date, eight samples have been tested and each repeated at least once. The results are shown in Figure 16 and Table 5. The samples supplied by ASD are listed with their compounding ingredients in Table 3.

Of these samples, 8A has the largest total expansion and also the lowest T_g; 12D has the highest T_g, and the others all fall within the upper half of the interval between these extremes.

The comparison of 12D and 12E seems to be of interest. The thermal expansion coefficient before and after their T_g's are similar, but the two values of T_g are about 15° apart. Assuming all other characteristics and processing to be the same, we find that 12D and 12E differ only in the monomer ratio of vinylidene fluoride

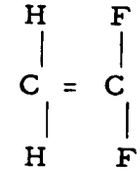

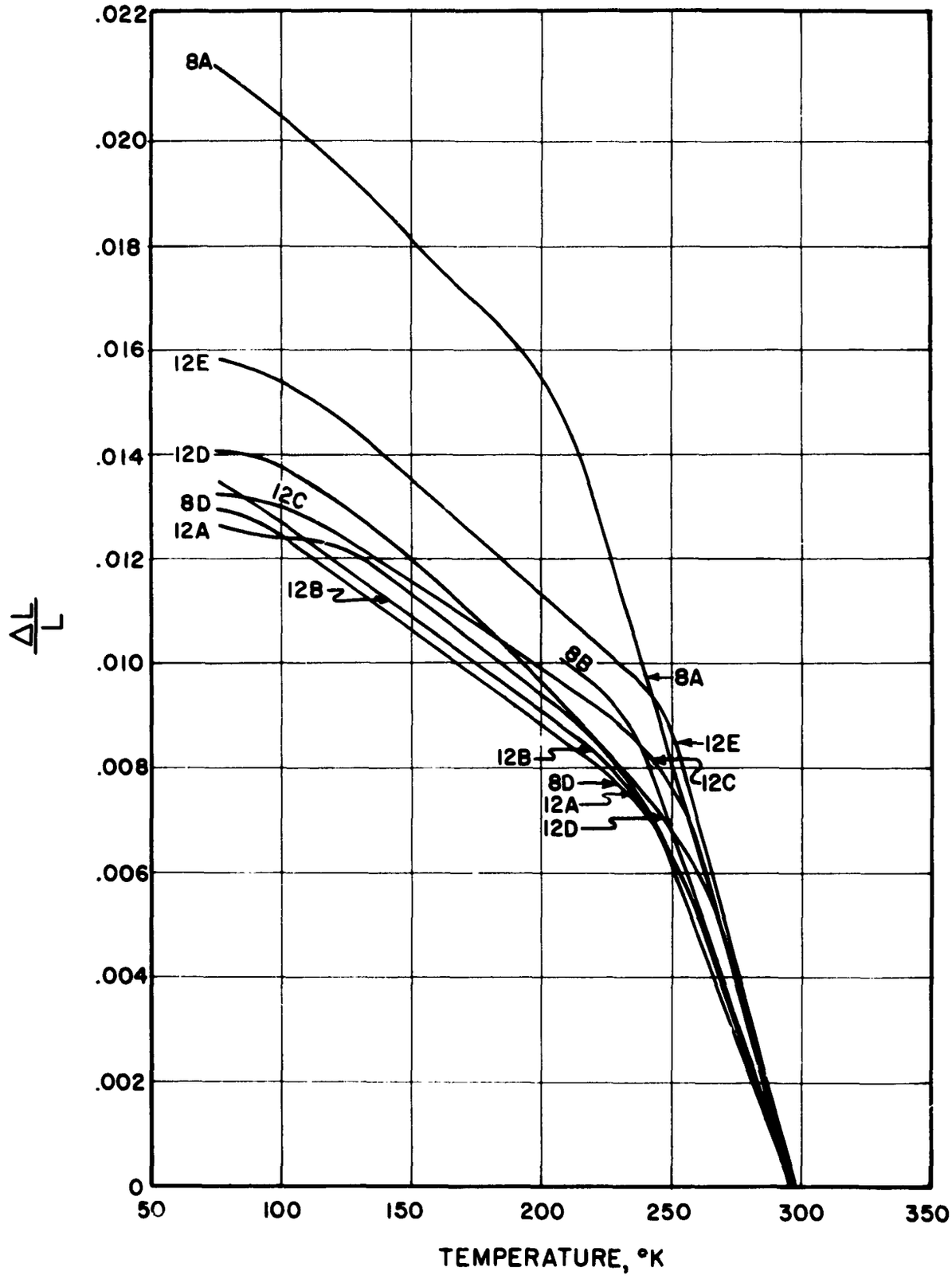

FIG. 16. Thermal Expansion of Elastomers

Sample No.	Expansivity below T_g $\frac{cm}{cm\ K°}$	T_g in °K	Expansivity above T_g $\frac{cm}{cmK°}$	$\frac{\Delta L}{L}$ from 297°K to 76°K
8D	3.6×10^{-5}	241	13.0×10^{-5}	12.9×10^{-3}
12B	3.6	241	13.0	13.5
12A	3.6	240	14.0	12.6
12D	4.5	262	18.6	14.1
12E	4.5	248	18.6	15.8
12C	3.3	249	17.9	13.2
8A	5.0	207	17.5	21.4
8B	3.5	234	14.6	14.5

Table 5. THERMAL EXPANSION AND T_g

and monochlorotrifluoroethylene 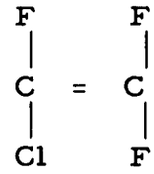 . If it is assumed that the chlorine and fluorine atoms in monochlorotrifluoroethylene are similar or more similar in size than the fluorine and hydrogen atoms are in vinylidene fluoride, then it can be seen that the configuration of 12D with a monomer ratio of 50/50 will be rougher and have available more "hooks" on its chains than that of 12E with a monomer ratio of 70/30. This may be one of the causes for the higher T_g of 12D, which results in lower total expansion even though the expansion coefficients of the two compounds are identical. Besides inhibiting the lengthening of the chains, the "hooks" may serve to capture other branches and hold them in close contact, enabling the molecules to act on one another with greater force. This may be a mechanism by which the units in these molecules are hindered in rotating, thereby resulting in a higher T_g in 12D than in 12E.

The comparison of 8D, 12B and 12C, all of which are copolymers of vinylidene fluoride and perfluoropropylene with monomer ratios of 70/30, and having the same compounding recipes, should be instructive. According to ASD, the molecular weight of 12B is greater than that of 12C, which in turn is greater than 8D, and all are between 60,000 and 100,000. It can be seen that the expansivities of 8D and 12B are very similar, with that of 12C larger in the temperature interval above T_g. Also, the T_g's of 8D and 12B are similar, with that of 12C slightly higher. From this information we see that molecular weight is not an important factor in influencing the T_g or thermal expansion, providing, at least in the case of T_g's [8] the molecular weight is large.

The terpolymer, 12A, has expansivity and T_g close to those of 8D and 12B with a curious flattening in the expansivity curve near 76°K.

Samples 12E (70 vinylidene fluoride/30 monochlorotrifluoroethylene) has a higher expansion than any of the vinylidene fluoride/perfluoropropylene polymers, although its T_g is close to that of 12C. Sample 12D has higher expansivity below 180°K and higher T_g than the others. This difference in expansion may be due in part to the

difference between the form of perfluoropropylene

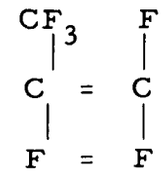

and monochlorotrifluoroethylene

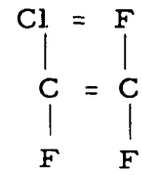

The former presents a jagged branch which would hinder movement, while the latter is smoother and presents a less obstructive form.

The above has been a preliminary examination of the results. These interpretations have leaned heavily on the form of the chain molecules. The effects of molecular forces such as the hydrogen bond and van der Waals force also have important influences, and these are marked for future study. We hope to probe deeper into the mechanisms of thermal expansion and second order transition by more study of the literature and careful analysis of our experimental results above and forthcoming.

3.4 Torsion Testing

3.4.1 Introduction

Early in the elastomer testing program it was decided that the low temperature stress-strain behavior of various rubber-like materials might be used to calculate low temperature seal behavior. With this in mind the deflection under compressive load at 76°K was measured using a representative sampling of elastomers and the results were reported[9, 17, 18]. Theoretically, the modulus calculated from these measurements should be identical with that derived from tensile stress-strain data if the deflection of the sample is sufficiently small. However, since frictional forces play a large (and unknown) part in any compression tests, an apparatus was designed to measure the strain when a sample is subjected to a torsional stress. This approach yields data which is free from frictional effects and has been used on metals and plastic foams at NBS[10, 11]. Samples having circular cross section were used, but Timoshenko[5] has shown that shear modulus can also be approximated from data based on rectangular samples by use of the following equation:

$$G = \frac{M_t}{k_1 \theta (2a)^3 (2b)} \qquad (1)$$

where

G = shear modulus, psi

M_t = applied torque, pound-inches

θ = twist angle per unit length, radians/inch

a = sample thickness, inches

b = sample width, inches

k_1 = a constant determined by a and b (values given in [12]).

Equation 1 yields a good approximation for G if b/a is at least 4. In our experiments b/a varied from 4.8 to 6.5; the use of equation (1) should therefore be valid. In this report results using available ASD sheet stock cooled to 76°K will be reported and discussed.

3.4.2 Apparatus and Experimental Procedure

Figure 17 shows the apparatus used for the tests. Two concentric stainless steel tubes are designed to accommodate elastomer samples clamped between them. The inner tube is allowed to rotate when weights are placed on the weight pans. The pans hang from fine nylon threads which run over pulleys to convert vertical force to horizontal torque. The torque is applied to the inner cylinder through a constant radius wing. The wing and inner tube are supported and aligned by three ball bearings riding in grooves. Twist angle is measured by reading movement of the wing on a circular scale scribed on the plate which supports the outer cylinder.

During a test the top plate rests on a dewar, and the test area is immersed in the coolant. Weights are placed on the pans and the resulting twist angle is measured. Hysteresis effects are reduced by cycling the load several times before the readings are taken. At least two tests were performed on each sample, and each reported test result is an average of several load applications. Twist angles are of the order of 2 to 10 degrees. The weight involved is around 1/2 pound, which applies about 1.5 pound-inches of torque to the sample. Sample dimensions are of the order of 0.5" x 0.08" x 2" free length.

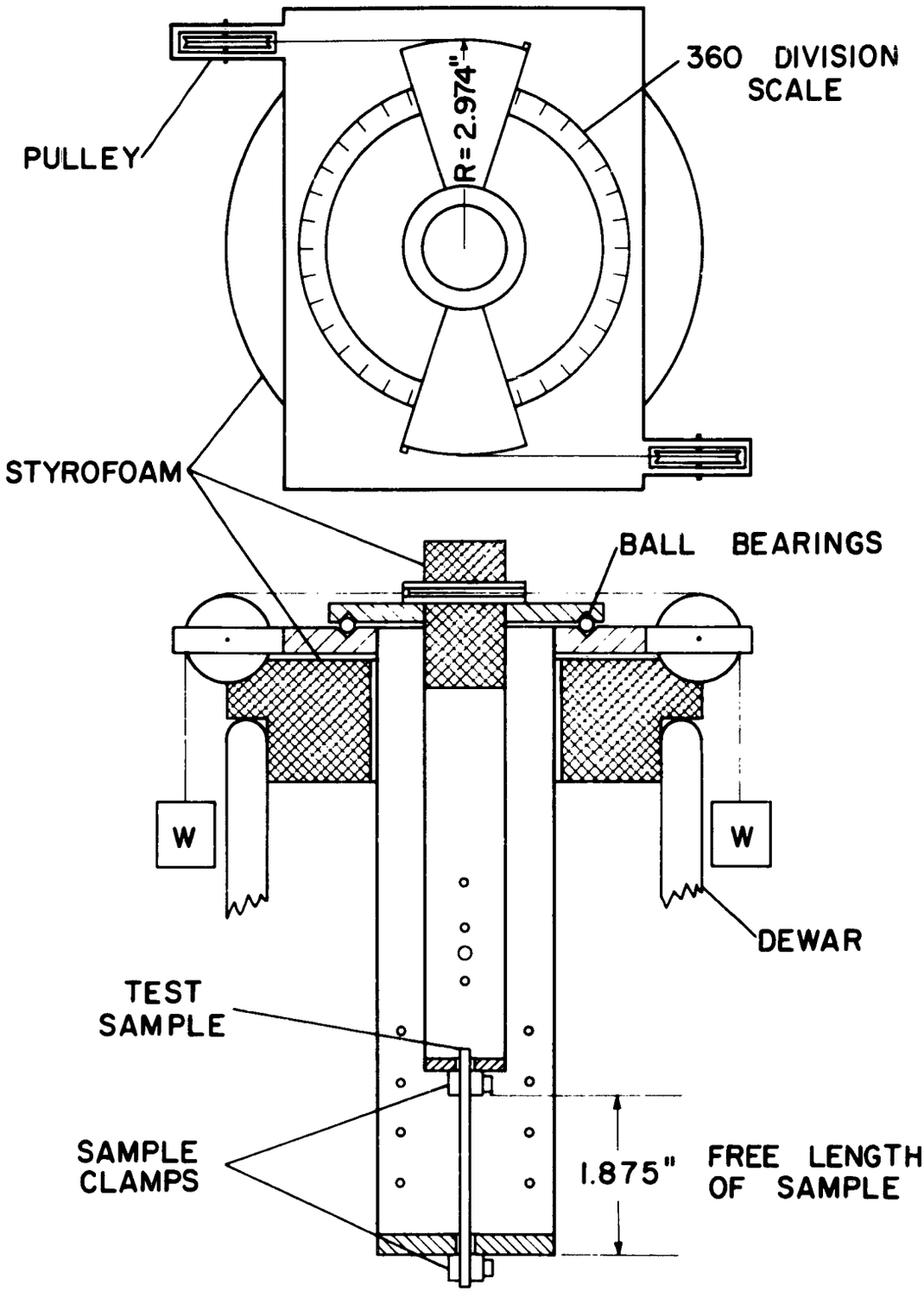

FIG. 17. Torsion Modulus Apparatus

3.4.3 Results and Discussion

Table 6 gives the 76°K shear modulus results using samples cut from sheet stock supplied by ASD.* The values given are within ± 5% of all test data available; since hysteresis effects were accounted for more reliably in later tests, the actual values may be on the low side of those reported. However, the test is intended to screen many compounds, and in all tests the comparative results on the various elastomers are as reported.

The results indicate that 21D and 21E are the softest compounds at 76°K with 8A, 21B and 21A also having shear moduli below 3×10^4 psi. However, the moduli of all materials tested are within a factor of 2. Assuming a Poisson's ratio of 0.25, the relation between G and Young's modulus E is:

$$E = 2.5G \qquad (2)$$

Values for E derived from Equation 2 are also given in Table 6. Compression tests using identical samples have not been made; however, comparisons with compression values taken with similar samples [9] indicate that the values derived from torsion measurements are lower by a factor of 3 or more, showing that frictional forces play a very significant role in the stress-strain properties of compressed elastomers at 76°K.

3.5 Differential Thermal Analysis

3.5.1 Introduction

A method commonly used to detect first and second order transitions in various materials is differential thermal analysis (DTA). A relatively recent book has been written on the subject [12], and a review article covers recent progress in the many applications of the method [13]. Basically, DTA measures the thermal effects when some transition results in a change in heat transport properties or heat capacity of a material. Usually these measurements are made while a sample is being heated or cooled at a constant rate, so that heat flux is constant throughout the experiment. However, since changes in state result in abrupt changes in the characteristic curves obtained by DTA, the heat flux need not be constant as long as no abrupt changes in heat flux occur.

In most polymer applications to date a differential thermocouple measures small differences between the sample temperature and that of an inert reference body which has similar heat transport

* Recipes and properties given in Table 7.

ASD No.	Polymer	Monomer Ratio	G (psi)	E (psi)
8A	Natural Rubber	---	2.47×10^4	6.19×10^4
18D	Isobutylene[A] and Isoprene	97.5/2.5	3.51	8.77
18D	Isobutylene and Isoprene	97.5/2.5	3.72	9.31
18C	Ditto	99/1	3.63	9.07
21D	Butadiene and Styrene	77/23	2.23	5.59
21E	Ditto	57/43	2.26	5.65
18B	Chlorinated Isobutylene and Isoprene	1/97/2	3.42	8.57
21F	Polyurethane	Unknown	3.57	8.92
21G	1, 1 Dihydroperfluorobutyl Acrylate	---	2.94[B]	7.38[B]
21B	Butadiene and Acrylonitrile	70/30	2.74	6.84
21A	Butadiene and Acrylonitrile	80/18	2.50	6.25

(A) Resin Cure
(B) During second test, material shattered while cooling

Table 6. TORSION TESTS AT 76° K

ASD No	Polymer	Estimated Monomer Ratio	Recipe		Original Properties			
					Tensile Strength (PSI)	Ultimate Elongation (%)	Hardness (Shore A)	Compression Set* (%)
21A	Butadiene and Acrylonitrile	80 18	Polymer	100	2050	400	75	8
			Zinc Oxide	5				
			Benzothiazyl Disulfide	1.5				
			Stearic Acid	1.5				
			Sulfur	1.5				
			FEF Carbon Black	50				
			Cure 20 min at 310°F					
21B	Ditto	70/30	Ditto 21A		2320	450	75	6
21D	Butadiene and Styrene	77/23	Polymer	100	1750	560	65	14
			Zinc Oxide	5				
			Benzothiazyl Disulfide	1.75				
			Stearic Acid	1.5				
			Sulfur	2				
			EPC Black	40				
			Cure 50 min at 320°F					
21E	Ditto	57/43	Ditto 21D		1930	580	70	25
21F	Polyurethane (Composition Unknown)		Polymer	100	2800	450	75	33
			Benzothiazyl Disulfide	3				
			Sulfur	1.5				
			"MBT"	1				
			Activator					
			$ZnCl_2$/MBTS Complex	0.35				
			HAF Carbon Black	30				
			Cure 30 min at 310°F					
21G	1,1 dihydro-perfluorobutyl Acrylate		Polymer	100	590	180	75	14
			Sulfur	1				
			FEF Carbon Black	40				
			Paraffin	1				
			Triethylene Tetramine	1.25				
			Cure 30 min at 310°F					

* 50% Compression, 90 hrs at room temperature

Table 7. RECIPES AND PROPERTIES OF ASD MATERIALS SUPPLIED FOR TORSION TESTING

ASD No	Polymer	Estimated Monomer Ratio	Recipe		Original Properties			
					Tensile Strength (PSI)	Ultimate Elongation (%)	Hardness (Shore A)	Compression Set* (%)
8A	Natural Rubber		Polymer (Smoked Sheet)	100	2200	350	65	10
			Stearic Acid	3				
			Zinc Oxide	5				
			N-cyclohexyl -2-benzothiazole sulfenamide	0.6				
			Sulfur	2.75				
			HAF Carbon Black	50				
			Polymerized Trimethyl-dihydroquinoline	1				
			Cure 15 min at 310°F.					
18B	Chlorinated Isobutylene and Isoprene	1/97/2	Polymer	100	2730	430	70	7
			Zinc Oxide	5				
			Stearic Acid	1				
			Benzothiazyl disulfide	0.5				
			Tetra methyl Thiuram Disulfide	1				
			Sulfur	2				
			HAF Carbon Black	50				
			Cure 30 min at 310°F					
18C	Isobutylene and Isoprene	99/1	Polymer	100	2320	740	70	8
			Ditto Additives 18B					
			Cure 30 min at 310°F					
18D	Isobutylene and Isoprene	97.5/2.5	Ditto 18C		2190	360	75	6

* 50% Compression, 90 hrs at room temperature

Table 7 (Continued) RECIPES AND PROPERTIES OF ASD MATERIALS SUPPLIED FOR TORSION TESTING

properties but has no phase changes in the temperature range of interest. The sample and the reference are cooled or warmed at the same rate, and any abrupt changes in the differential between the two indicates a first or second order transition in the sample. A somewhat simpler approach to DTA has been reported recently[14]. This more recent method, which eliminates the reference material by measuring the thermal lag in the sample, has been incorporated into the elastomer program and will be continued through the coming year. At this time the apparatus will be described and preliminary data obtained with a natural rubber sample supplied by ASD will be discussed.

3.5.2 Apparatus and Experimental Method

It was decided that the simplest and most meaningful method of measuring the thermal effects in an elastomer would be to measure the temperature difference between a point near the center of the sample and a point near the surface. Although small, this difference will always exist when heat is being transferred into (or out of) the system. In the Figure 18, the differential thermocouple is shown in test position. To position the copper-constantan thermocouple in the 1/2" diameter x 1/2" long sample, the wires are first threaded through the sample with a sewing needle, the needle is removed, and the junctions are adjusted to be in the proper position. An additional thermocouple is positioned on the exterior of the sample to read the sample temperature, using room temperature as the reference.

The sample is suspended by the thermocouple wires from a support tube, which passes through a vacuum coupling. The coupling is soldered directly to the upper tube of a vacuum-tight can which surrounds the sample area. The can is copper, to insure uniform heat transfer to all surfaces of the sample. The thermocouple wires leave the vacuum area through a wax seal. A fore and diffusion pumping system is available to keep the sample area free from most condensibles. The sample temperature is indicated by a small portable potentiometer which is manually read at the time of any significant event during a test. The differential across the sample is amplified, and a voltage divider is incorporated in order to reduce the stray emf generated by the amplifier. The differential is partly counterbalanced by a bucking potentiometer, in order to keep the signal on scale and obtain a highly magnified picture of events taking place. This instrumentation is good enough to indicate a one micro-volt change of differential as full scale (ten inches) change on the 10 millivolt recorder; however, the present cooling rates do not allow the full

EXPERIMENTAL SET-UP INSTRUMENTATION

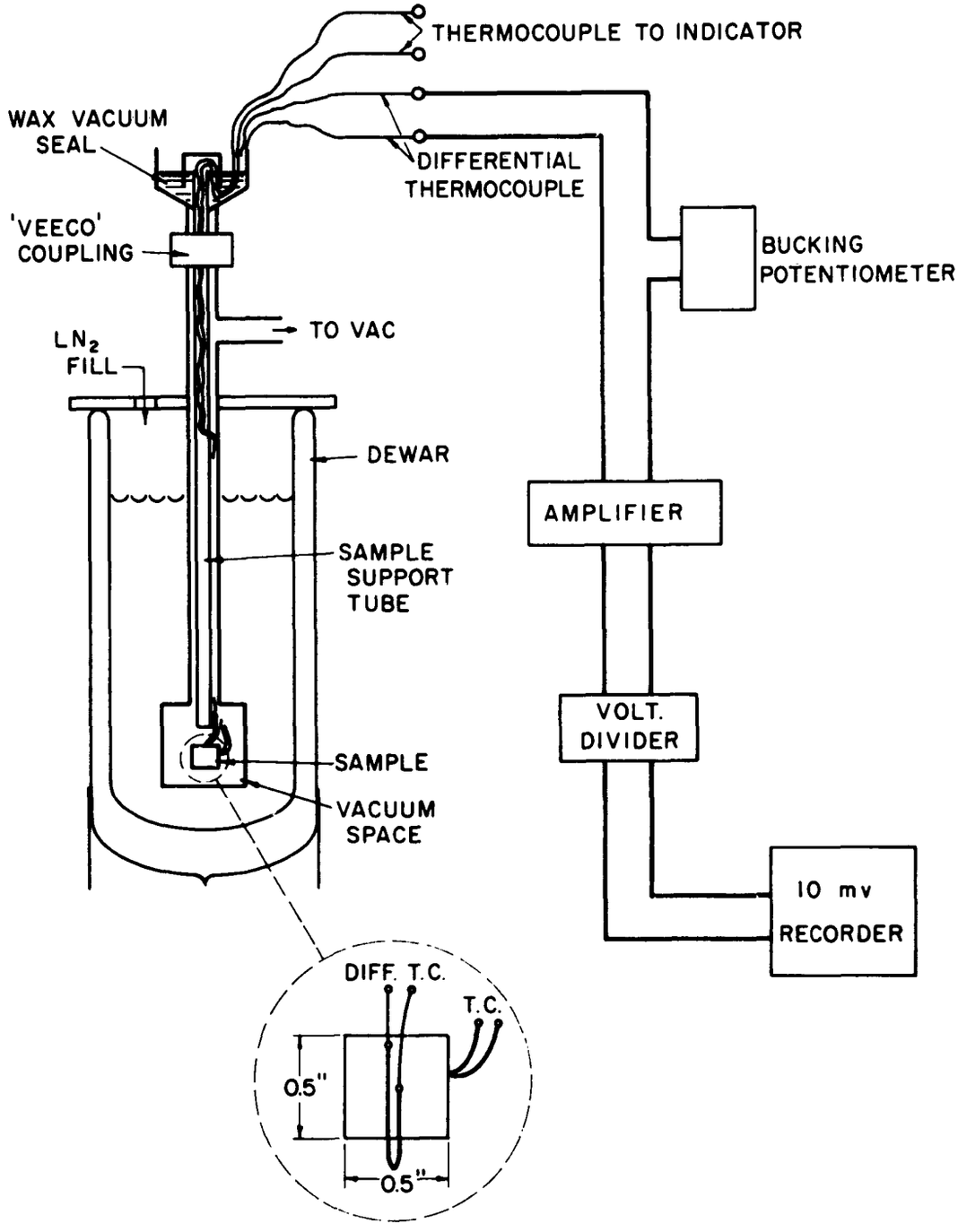

FIG. 18. Differential Thermal Analysis

sensitivity of the system to be utilized.

To allow a reasonably stable condition prior to a test, the apparatus is immersed in liquid nitrogen and allowed to cool over night. For preliminary testing the procedure has been to allow the system to warm to 150°K before the differential measurements are commenced. Heat transfer rates are higher between 76°K and 150°K, and conditions are not very close to steady state. Also, radical changes are not expected in the lower range. When the sample reaches 150°K, the recorder is turned on and a continuous record of the differential is recorded while the sample warms to 280°K. Above this temperature the warming rate is very slow, and a heater will have to be used to make measurements practical.

3.5.3 Results and Discussion

Results of a preliminary test to demonstrate the type of information available using DTA techniques is shown in Figures 19 and 20. The natural rubber used for the test was obtained from ASD, and the compounding recipe is given in Table 7. In Figure 19, two curves are shown to illustrate the complete test. The dotted line refers to the warming rate of the sample, which shows a smooth, steadily decreasing rate except for the area around 240°K. At this temperature the rate slows almost to zero for a short time, then recovers and continues as before. This indicates that either the heat input to the sample was interrupted for a short time, or the sample underwent an endothermic transition of some sort, such as the melting of crystals previously formed. Further description of the behavior around 240°K is shown by the differential curve on the same figure, which plots the differential potential between the two copper constantan junctions. Since the sample is warming, the differential is considered positive when the outer temperature is warmer than that of the inner volume. At about 240°K a very abrupt increase in differential is noted, increasing ΔE by about 50 micro-volts, or 2°K. We remember, however, that the warming rate of the exterior of the sample decreased in this area. Therefore the center volume must have cooled in this region, indicating strong melting at 240°K. This melting peak was not expected until about 284°K, as reported by Dannis[14] in a similar experiment using both pale crepe and smoked sheet natural. However, it has been shown[15, 16] that the temperature range in which melting of crystals occurs depends on the temperature at which crystallization takes place, and further it was found that melting commences when the temperature is 4-6 K° higher than the temperature of crystallization. For this consideration to adequately explain the sharp melting peak

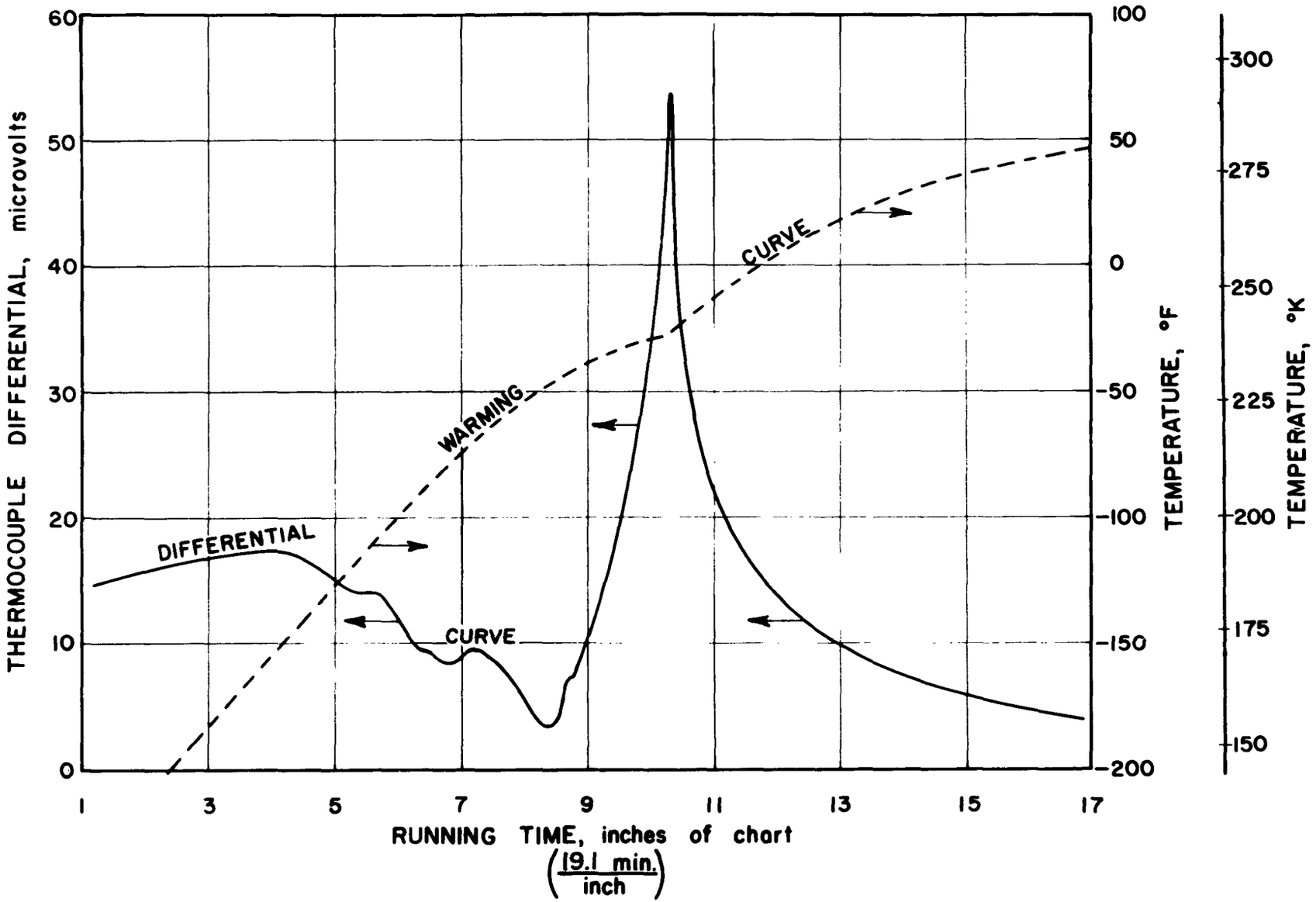

FIG. 19. Differential Temperatures and Warming Curve, Sample 8A

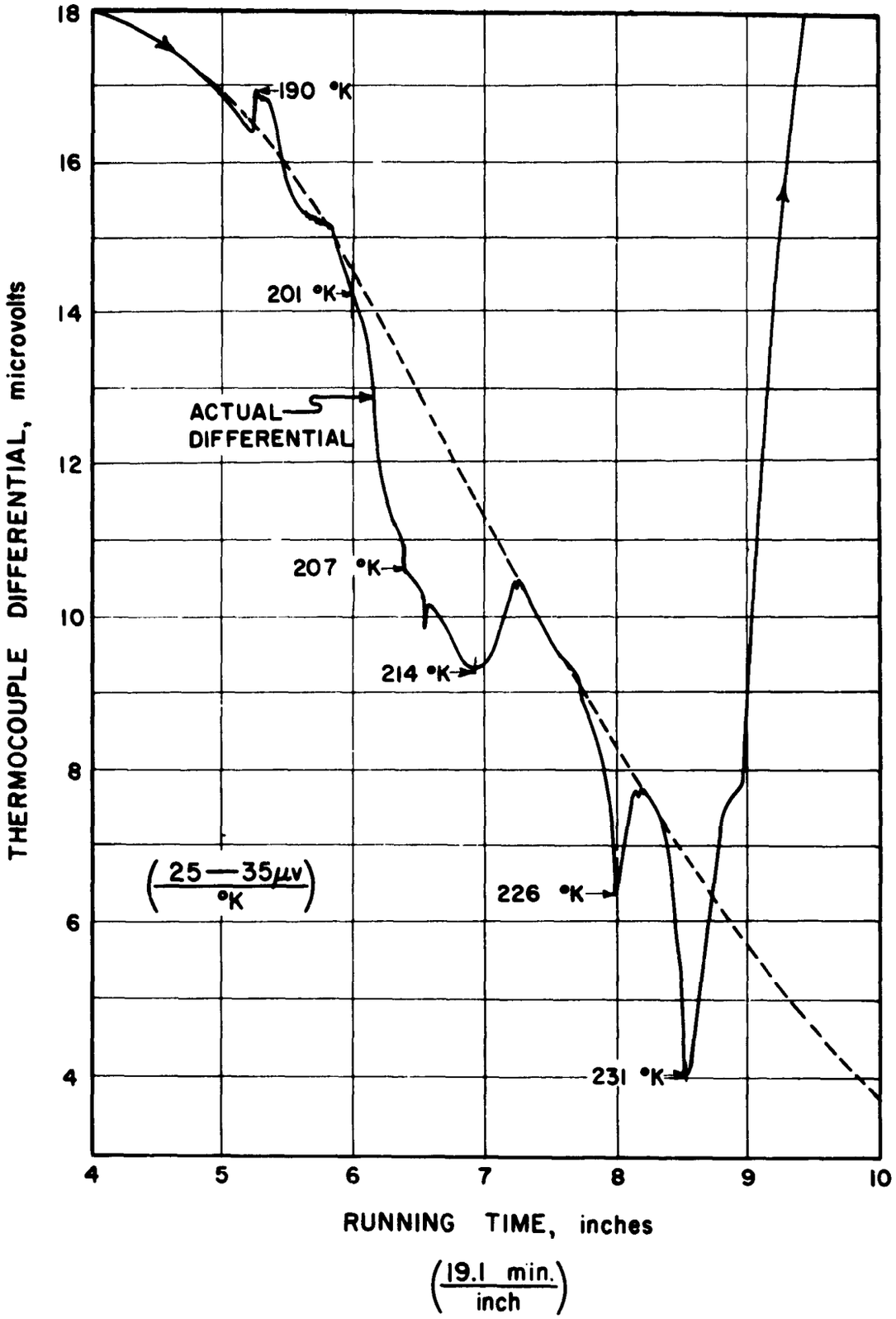

FIG. 20. Differential Temperatures in Sample 8A

observed, it would be necessary to have a large portion of the crystallization to take place around 230°K. Since the cooling rate of the sample was uniform, it was instead expected that the crystal would melt slowly and no sharp melting climax would be observed. The results are preliminary in nature and possibly other factors not yet considered are responsible for this phenomenon. Although we cannot be sure of the validity of the sharp melting peak at present, further tests may give additional stature to this quite unexpected result.

At temperatures below 240°K several additional events take place. These are not well defined in Figure 19; however, the original data, as shown in a direct tracing in Figure 20, are more clearly defined. It should be noted that a one micro-volt change in differential corresponds to a change in ΔT of 0.03 to 0.04K°, depending upon the temperature of the measurement. Between 190 and 201°K the glassy state transition is indicated, although this event was expected between 200 and 210°K. Since the temperature-indicating thermocouple used a room temperature reference, it is possible that variations in room temperature caused the temperature indication to be slightly low throughout the test. Between 201 and 214°K the curve dipped sharply, showing formation of crystals in addition to those formed during cool-down. After this crystallization the curve continued on the hypothetical "normal" curve shown by the dotted line for about 10 degrees, where further crystallization, and probably some melting at about 228°K, were events preceding the proposed melting peak at 240°K.

Additional comments on the above phenomena will be reported in future reports, as we become more familiar with DTA and the primary and secondary transitions in elastomers.

3.6 Compression Testing of Some Composite Inorganic Seal Materials

The Armour Research Foundation materials testing laboratory has investigated the possibility of combining the structural properties of hard metals with the conforming properties of soft, ductile metals to be used primarily for high temperature seals. In coordination with this effort N.B.S. - C. E. L. has tested several compounds supplied by Armour to determine their low temperature behavior. Sealability tests have been reported previously. In brief, it was found that gaskets containing the metal indium as the soft impregnate made leak tight high vacuum, high pressure seals at temperatures as low as 20°K. The testing conditions and flange designs were similar to those previously used in the functional elastomer seal tests.

The promising results obtained from these tests prompted preliminary investigations of the mechanical and viscous behaviors of the composites, at room temperature and at 76°K. It is hoped that comparisons between results at various test temperatures will aid in understanding the composite structure and its possible use for low temperature seals.

TABLE 8 COMPOSITE INORGANIC TEST SPECIMENS

Sample	A	B	C	D	E
Skeleton	430 ss*	430 ss	304 ss	Molybdenum	430 ss
Skeleton bonded?	Yes	Yes	Yes	Yes	No
Skeleton density	23%	23%	22%	31%	23%
Impregnate	indium	indium	indium	silver	silicone resin slurry

* Stainless Steel

3.6.1 Materials and Apparatus

The five samples tested were supplied by Armour; they are designated A, B, C, D, E in Table 8 and were cylindrical (approximately 1 in^2 x 1/2 in. long) before testing. Since only a limited number of tests could be performed on each sample, stress-strain curves in compression and load relaxation were chosen to describe the behavior of the materials. Tests were performed using an Instron universal testing machine and graphs of applied load vs. time were made using the Instron recorder. Crosshead speed was maintained at a constant rate of 0.002 inches per minute during all tests.

Figure 21 shows the compression cryostat and loading members. The overall deformation was calculated from the relative time rates of the chart and the crosshead. Deformation of the loading members was measured, and subtracted from the overall to determine the actual sample deflection. The loading members were responsible for more than 60% of the total deflection in most cases; consequently the measurements are not quantitatively accurate. This is particularly true at stresses less than 200 psi. In order to use the Instron machine directly in compression a load cell was mounted on the bottom of the moving crosshead, and the compression cryostat was placed on a large plate mounted on the base of the machine.

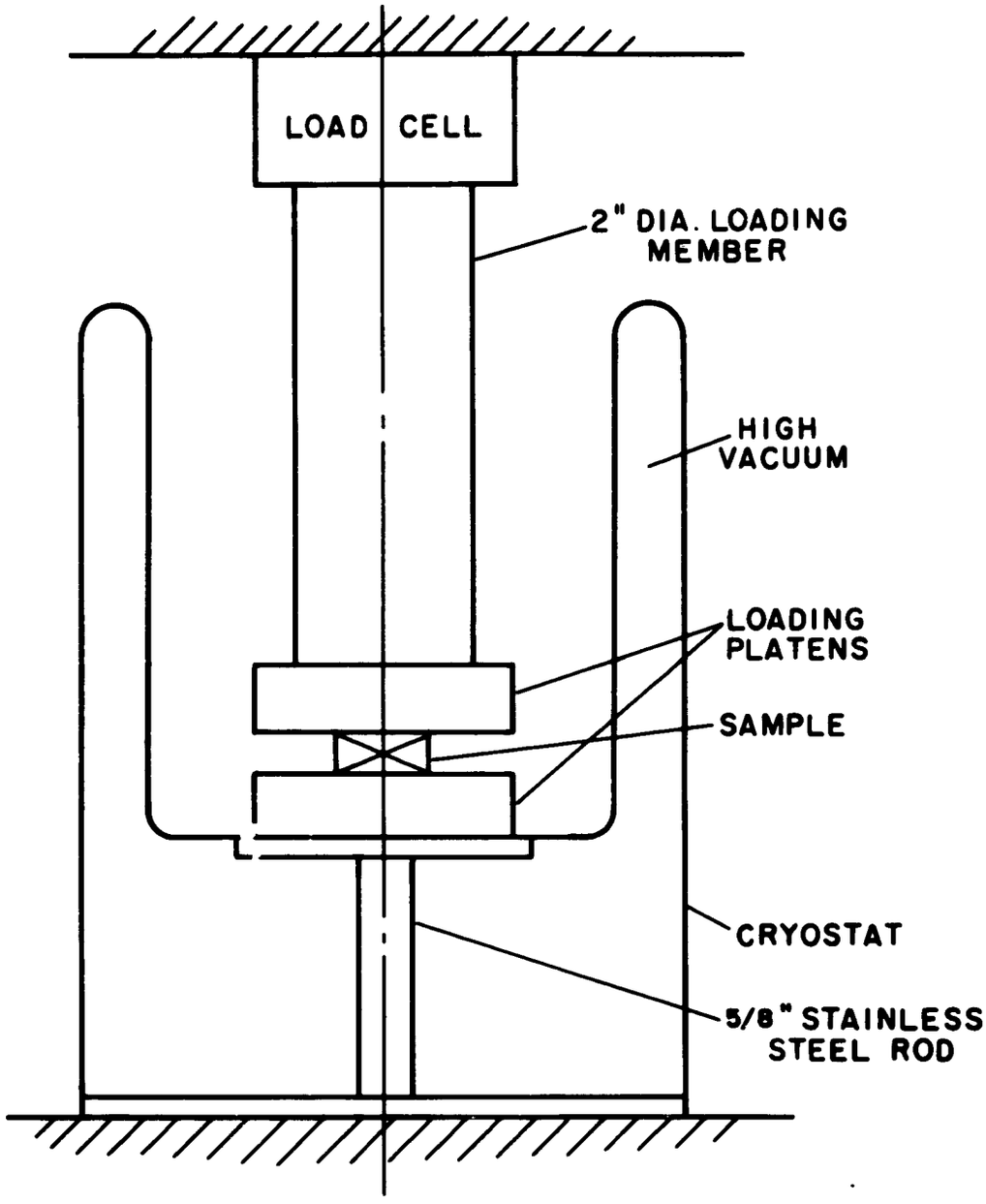

FIG. 21. Compression Cryostat and Loading Members

3.6.2 Testing Procedure

Two samples of the 430 ss + indium composite and one each of the other three composites were available for testing; therefore more tests were performed on the 430 ss + indium than on the others. The tests were performed and reported by T. F. Durham of the Mechanical Properties section of the N. B. S. Cryogenic Engineering Laboratory. The deformations refer to total deflection. Thus "the sample was deformed 5%" means that the total deformation of the sample and the loading rods was 0.05 x 0.5 = 0.025 inches. Following is Mr. Durham's report of test procedure on each sample:

Specimen A: Nominally 0.505" thick with a diameter of 1.130". All loads were applied at room temperature and the sample was deformed successively to 1%, 5% and 20% deflection with stress relaxation curves of 1 minute duration and unloading curves obtained for each test. Final thickness of the specimen was 0.417 inches. The sample was then reloaded to obtain a stress relaxation curve of 10 minutes at 20% deflection. No further measurements were made.

Specimen B: Nominally 0.505" thick with a diameter of 1.130". All loads were applied at 76°K and the sample was deformed successively to 5% and 6%. Stress relaxation curves of 1 min. and 6-1/2 min., respectively, and unloading curves were obtained. Deforming this sample beyond 6% would have involved loads much greater than 5000 lbs and this was considered undesirable with the particular loading apparatus being used. Also the sample was thought to have been deflected to 1% but this amount was later found to be "take up" in the loading members. On all subsequent tests this "take up" was compensated for. The sample was permanently deformed 0.012".

Specimen C: Nominally 0.505" thick with a diameter of 1.130". At room temperature the specimen was deformed 1%. It was then cooled to 76°K and again deformed 1%, and following this it was deformed 5%. Stress relaxation curves of sufficient duration to establish the behavior, and unloading curves were obtained for each test. After warmup the specimen was found to have sustained only about 0.001" permanent deformation.

Specimen D: Nominally 0.502" thick with a diameter of 1.130". At room temperature the sample was deformed 1%. It was then cooled to 76°K and deformed successively 1%, 5% and again 1%. Stress relaxation curves for periods up to 20 minutes,

and unloading curves were obtained for all tests. After warm-up the specimen was found to have sustained only about 0.001" permanent deformation.

Specimen E: Nominally 0.502" thick with a diameter of 1.130". The specimen was deformed 1% at room temperature and then 1% and 5% at 76°K. Stress relaxation curves for periods of about 3 to 10 minutes and unloading curves were obtained. There was approximately 0.003 inches permanent deformation.

3.6.3 Discussion of Results

Since the deformation of the loading members played an important part in the total deflection recorded on the original graphs, the data were translated to working curves and these corrected curves plotted in Figures 22 thru 27. In all cases the stress was calculated on the basis of the initial cross section area of the sample.

Figure 22 shows room temperature loading curves for each sample. Only sample A was loaded extensively at room temperature, and a complete curve for this test is shown in Figure 23. With reference to Figure 22, it should be re-emphasized that difficulties in measuring the exact deformation of the loading members in this range of loads cause some doubt as to the quantitative value of the curves. However, the shape of the curves should be valid. The steadily increasing slope was not observed in tests by Armour at room temperature shown in WADC Tech. Report 59-338, Part I. The increasing slope in the NBS curves (Figure 22) is probably due to two effects not representative of the materials as a whole. These are 1) initial compression of surface irregularities, which reduces the actual loading area; 2) compression of a film of the soft impregnant which is closest to the surfaces. In other words, the main body of the sample does not "see" the entire applied load until these initial effects have been overcome. However, they cannot be disregarded, since they are present each time a sample, or a gasket type seal, is compressed at room temperature. The strain rate also plays an important role in the measurements. The curves might have entirely different characteristics if the strain rate were increased or decreased by a factor of five. This could also be a reason for discrepancies between the NBS tests and the Armour tests. The Armour tests were taken with a constant rate of stress during the loading period, whereas the present testing used a constant rate of strain.

Figure 23 shows two tests run on sample A at room temperature, including the unloading portion of the second test. Hysteresis in the loading rods prevented accurate analysis of the unloading curves in general; however, in Figure 23 the deformation was much greater

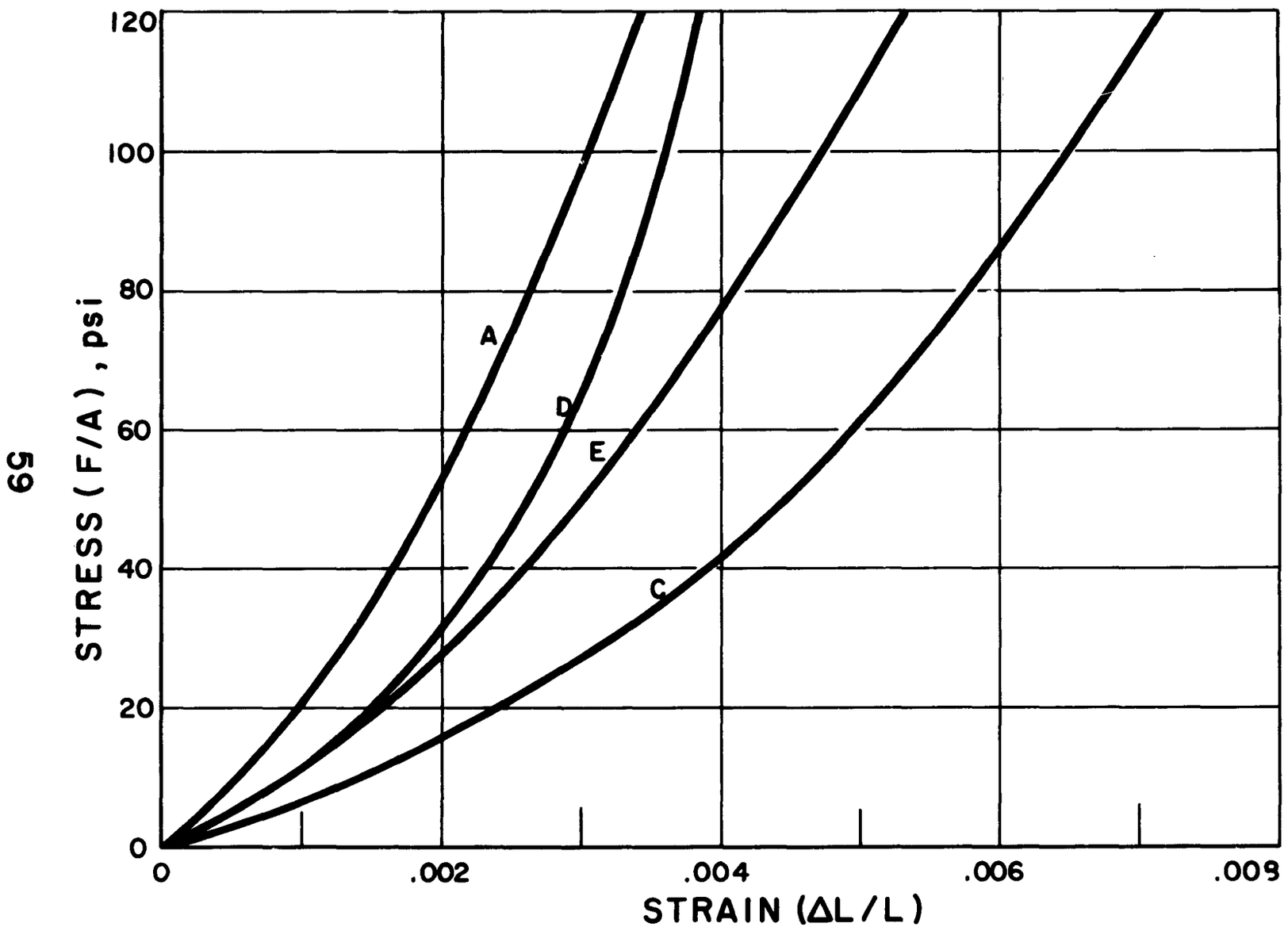

FIG. 22. Room Temperature Compression Loading of Inorganic Composites

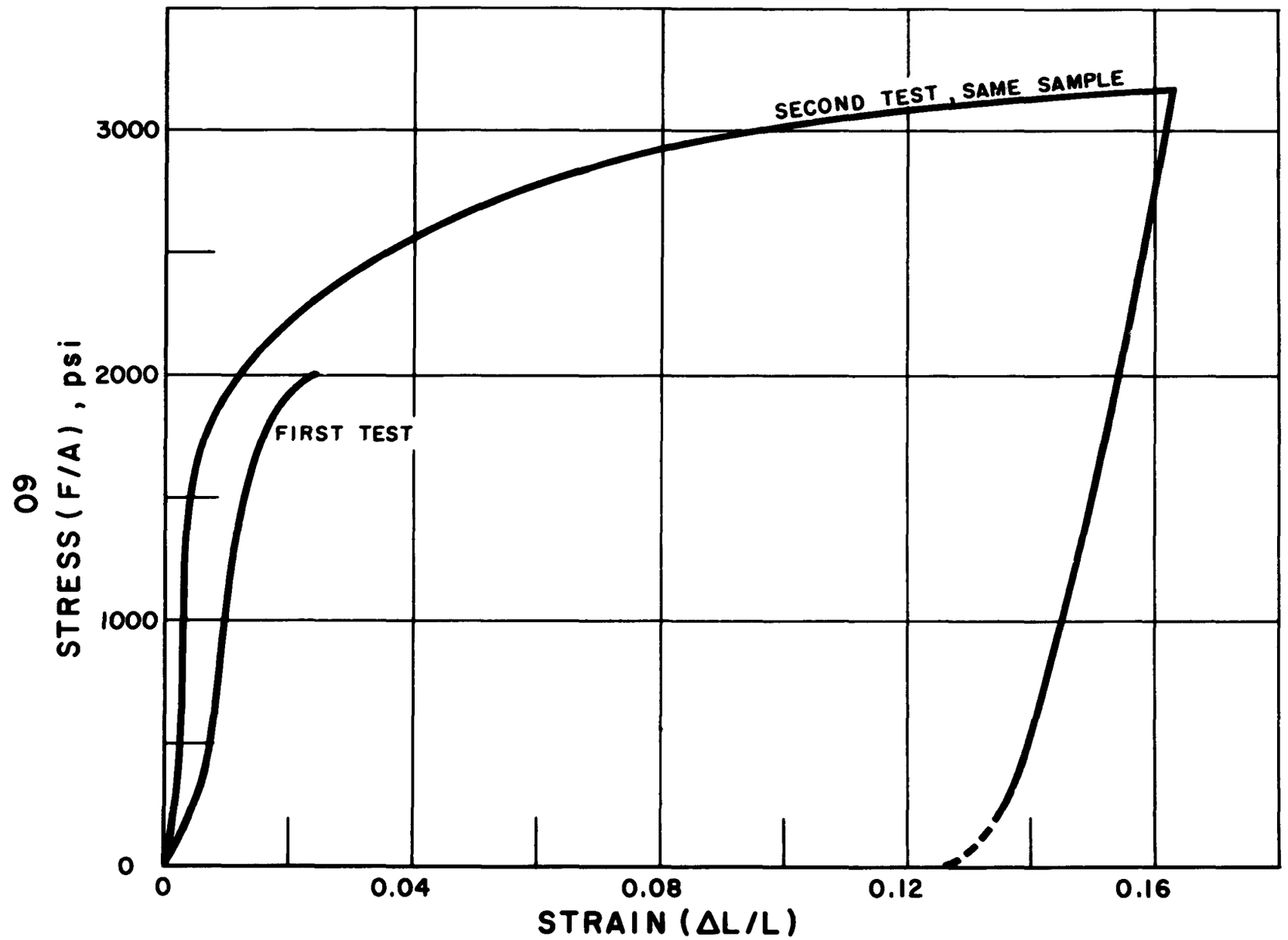

FIG. 23. Loading and Unloading of Sample A at Room Temperature

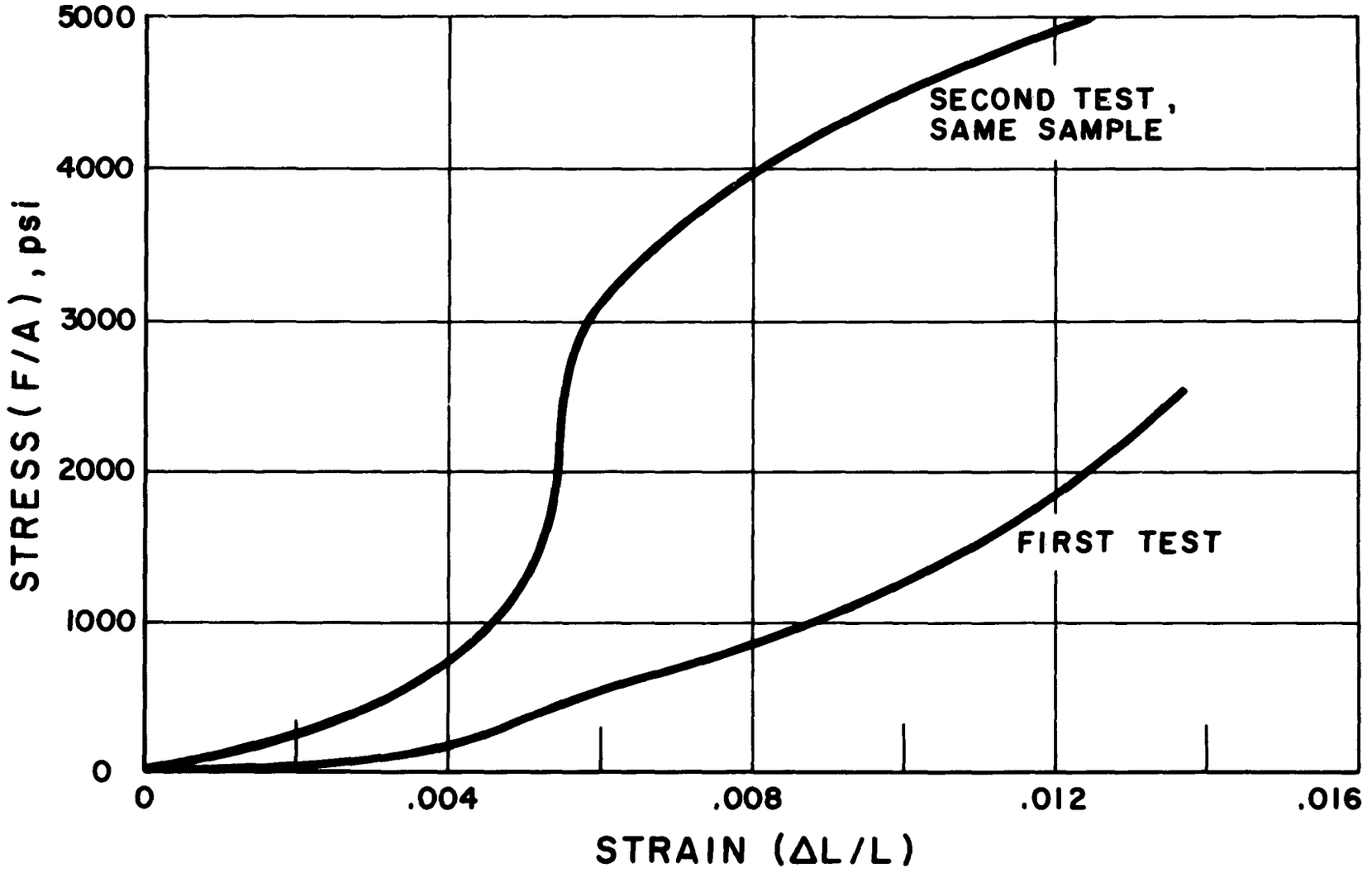

FIG. 24. Loading Curves of Sample B at 76 °K

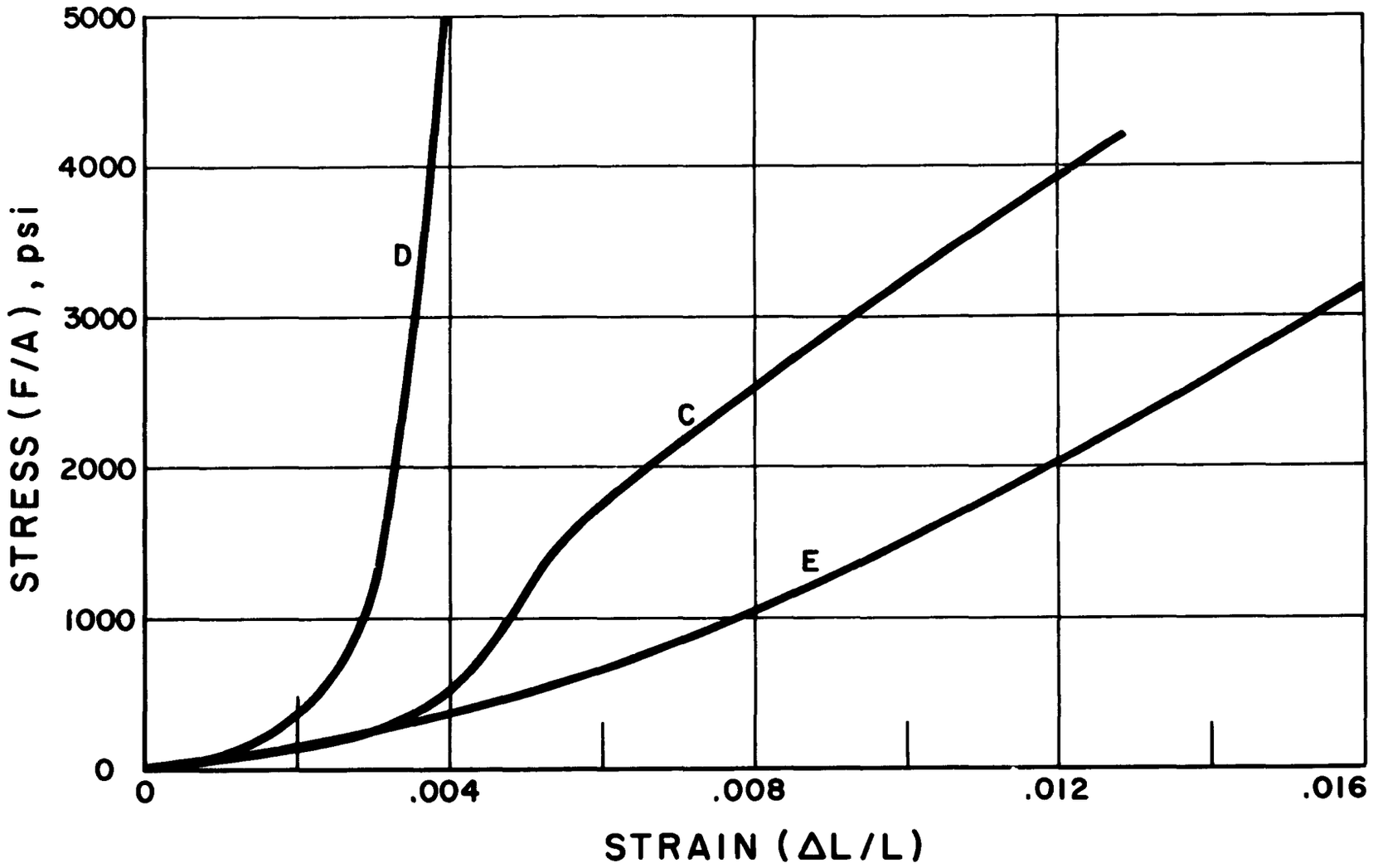

FIG. 25. Loading Curves for Samples D, C, and E at 76 °K

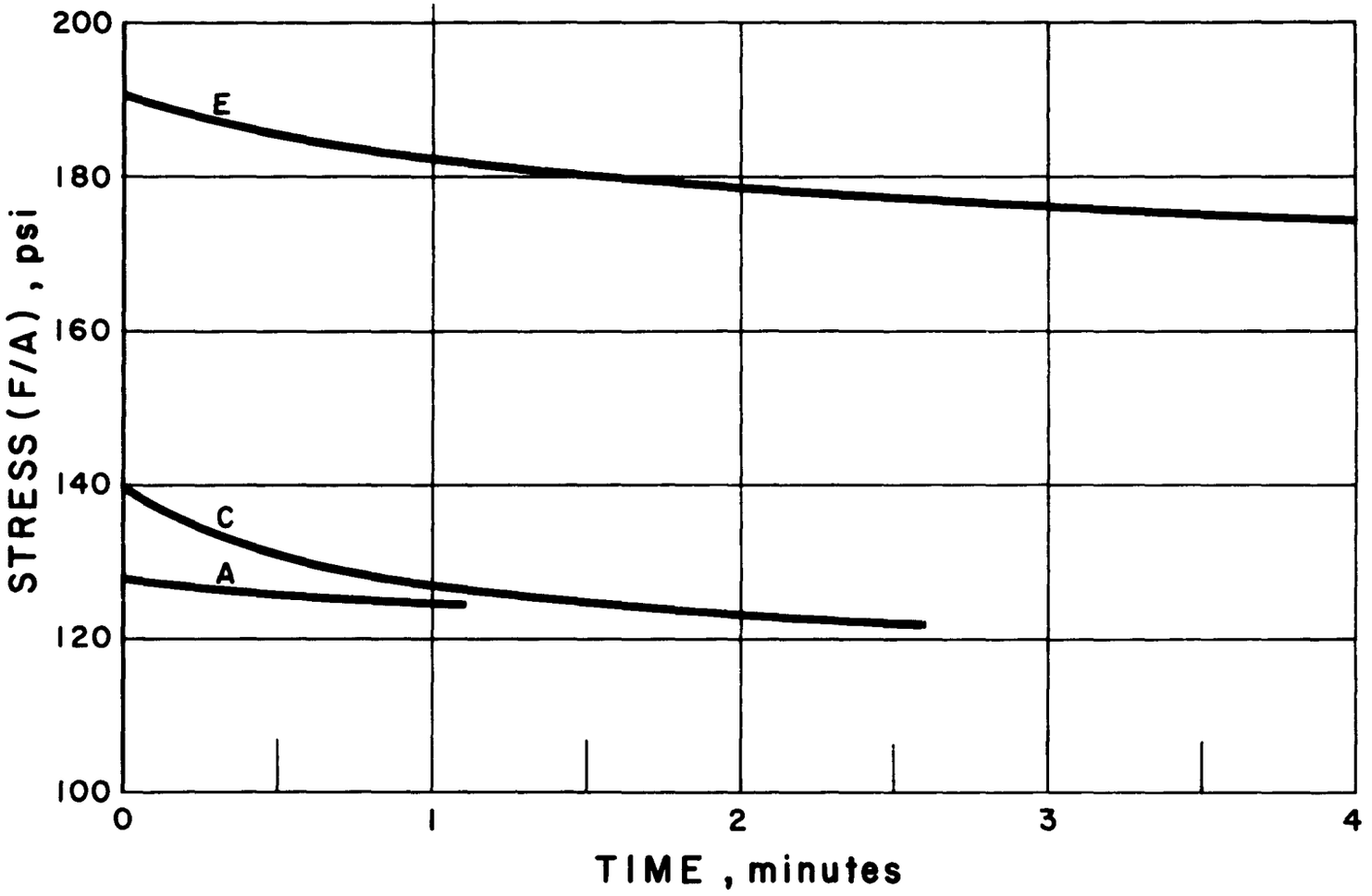

FIG. 26. Relaxation of Compressed Composites at Constant Strain, Room Temperature

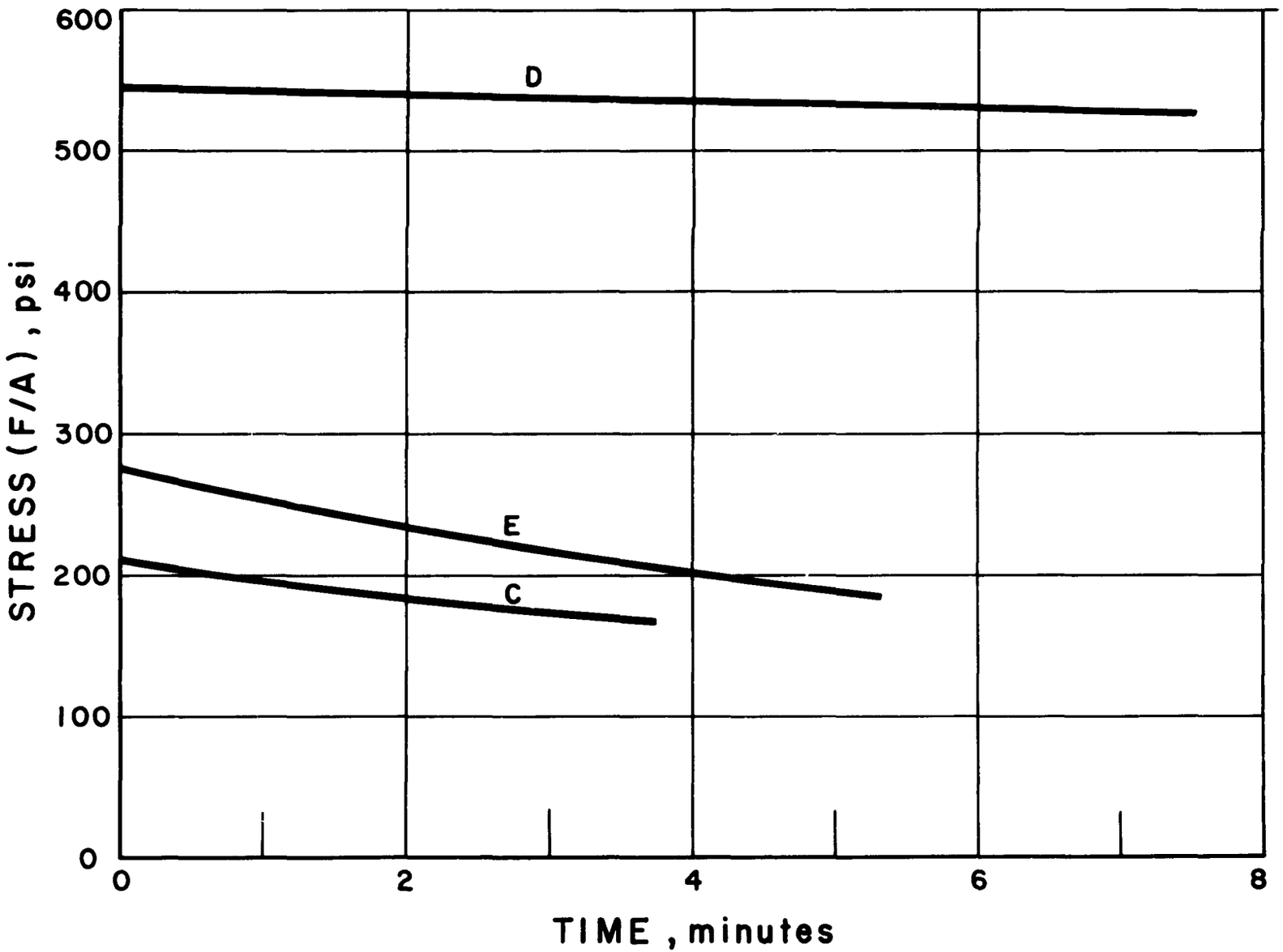

FIG. 27. Relaxation of Compressed Composites at Constant Strain, 76 °K

than that for other tests, and some analysis of the recovery was possible. Note that stress was calculated on the basis of the initial cross section of the sample, not a good approximation for this test since the area increased significantly during the loading period. Note also the yield for both tests, and the non-recoverable plastic flow after yield for the second test.

Figures 24 and 25 show loading curves taken at 76°K. The curve for sample C, 304 ss + indium, was actually the second test performed on the sample, and therefore can be compared with the second test performed on sample B, 430 ss + indium. It can be seen that the stronger 430 skeleton caused a higher yield strength, but after yield the indium was the more predominant material and the slopes of the curves were similar. Sample D did not show a yield, probably due to the greater skeleton density and higher strength of the impregnate. The non-bonded skeleton of sample E was not as strong, and behaved in a manner similar to the post-yield curves of samples B and C. Permanent deformation was somewhat greater for this sample, but even so, most of the deflection was recovered.

After a seal has been assembled, it is important that most of the initial sealing force be maintained throughout the use of the seal. Hence some knowledge of the viscoelastic behaviors of the composite inorganic seal materials is important to the design engineer. To this end stress relaxation at constant strain was measured as a function of time during the stress-strain tests described above. Figures 26 and 27 show the results of these tests at room temperature and at 76°K, respectively. Sample D was omitted from Figure 26 because no relaxation was measured from a stress below 200 psi; however, the relaxation was very small - from 450 psi to 435 psi in 4 minutes, with a shape similar to that of sample E, Figure 26. Sample B was omitted from Figure 27 because irregularities in the testing procedure are believed to have affected the results.

4. Summary and Plans

It has been shown by the above work that standard o-rings of ordinary elastomeric polymer compounds can be used for high performance seals at cryogenic temperatures. Very satisfactory seals have been obtained with several elastomers, including neoprene and natural rubber. Simple flat flanges are suitable if used with highly compressed o-rings of small cross section.

These results are somewhat unexpected in the light of accepted ideas regarding the properties of elastomers at extreme low tempera-

tures. It is well known, for example, that polymers have high expansivities and become glass-like below characteristic transition temperatures. These properties might lead one to expect that elastomers clamped between metal flanges cannot retain a seal at cryogenic temperatures. The fact that o-ring seals have nevertheless remained strong and tight far below their brittle point emphasizes the need for a better understanding of changes in physical properties throughout the low temperature range.

The work to date has shown that there are no simple correlations between seal performance and expansivity, brittle point temperature, or compression and shear modulus at 76°K. The measurement of these properties, and others, from above the brittle point to cryogenic temperatures is nevertheless very valuable and will eventually enable us to explain and predict the performance of elastomers as seals. Thermal expansivity measurements will continue to receive important emphasis and an attempt will be made to determine shear modulus and compression modulus at all temperatures between the brittle point and 76°K. The force evaluation experiment will yield diagrams of the forces exerted by an o-ring during cooldown and while functioning as a seal. Other information, continuous with temperature, will be obtained from DTA measurements, as described above, and a rebound experiment which is in the design stage. It is hoped that most of these properties can eventually be correlated with seal performance, with polymer variation, and with compounding parameters.

REFERENCES

1. Walker, W. R., Design Handbook for O-Rings and Similar Elastic Seals, WADC Technical Report 59-428, Part II (1961)

2. Martin, G. M., Roth, F. L., and Stiehler, R. P., Behavior of Pure Gum Rubber Vulcanizates in Tension, Trans. Inst. Rubber Ind. 32, 189 (1956)

3. Payne, A. R. and Scott, J. R., Engineering Design With Rubber, Interscience Publishers, Inc., New York (1960)

4. Treloar, L. R. G., The Physics of Rubber Elasticity, Clarenden Press, Oxford, England (1958)

5. Timoshenko, S., and Goodier, J. N., Theory of Elasticity, 2nd Ed., McGraw-Hill (1951)

6. Schmidt, A. X., and Marlies, Principles of High Polymer Theory and Practice, 89, McGraw-Hill (1948)

7. Spencer, R. S., and Boyer, R. F., Journal of Applied Physics 17, 399 (1946)

8. Reference [6], 193

9. Weitzel, D. H., Robbins, R. F., Bopp, G. R., Elastomers for Static Seals at Cryogenic Temperatures, Advances in Cryogenic Engineering VI (K. D. Timmerhaus, Editor), Plenum Press (1961)

10. McClintock, Low Temperature Properties of Plastic Foams, Soc. Plastics Engineers J., 14, No. 11 (1958)

11. Mikesell, R. P., Unpublished Data, NBS-Cryogenic Eng. Lab.

12. Smothers, W. J., Chiang, Y., Differential Thermal Analysis, Theory and Practice, Chemical Publishing Co., Inc., New York (1958)

13. Murphy, C. B., Anal. Chem 32, 168R (1960)

References (continued)

14. Dannis, M. L., Transition Measurements Using Differential Thermal Analysis (DTA) Techniques, Presented at 140th Am. Chem. Soc. Meeting, Chicago (1961)

15. Treloar, L. R. G., The Physics of Rubber Elasticity, Clarenden Press, Oxford, England (1958)

16. Wood, L. A., Advances in Colloid Science, II, 57, Interscience, New York (1946)

17. Robbins, R. F., Weitzel, D. H., Herring, R. N., The Application and Behavior of Elastomers at Cryogenic Temperatures, Presented at 7th Cryogenic Engr. Conf, Ann Arbor, Mich. (1961)

18. Trepus, G. E., Roper, R. S., Hickman, W. R., Design Data for O-Rings and Similar Elastic Seals, WADC Tech. Report 56-272, Part IV and V (1959, 1960)

GPO 854396

NATIONAL BUREAU OF STANDARDS, Boulder, Colorado. ELASTOMERIC SEALS AND MATERIALS AT CRYOGENIC TEMPERATURES, by D. H. Weitzel, R. F. Robbins, P. R. Ludtke, Y. Ohori, R. N. Herring,

68 p. incl. figs., tables and refs. (Project 7340; Task 73405) (ASD TDR 62-31) (Contract AF 33(616)-61-04)

Unclassified report

This research deals with investigations of elastomeric polymers, with particular emphasis on their usefulness as seals at cryogenic temperatures. O-ring seals utilizing various flange configurations

(over)

UNCLASSIFIED

UNCLASSIFIED

have been extensively evaluated at temperatures between 76 and 300°K. A supporting program of property measurements includes thermal expansivities, shear and compression modulus, differential thermal analysis, and the force-temperature effects of prestressed elastomers. O-rings and other specimens have been prepared and supplied by Aeronautical Systems Division.

UNCLASSIFIED

UNCLASSIFIED

NATIONAL BUREAU OF STANDARDS, Boulder, Colorado. ELASTOMERIC SEALS AND MATERIALS AT CRYOGENIC TEMPERATURES, by D. H. Weitzel, R. F. Robbins, P. R. Ludtke, Y. Ohori, R. N. Herring,

68 p. incl. figs., tables and refs. (Project 7340; Task 73405) (ASD TDR 62-31) (Contract AF 33(616)-61-04)

Unclassified report

This research deals with investigations of elastomeric polymers, with particular emphasis on their usefulness as seals at cryogenic temperatures. O-ring seals utilizing various flange configurations

(over)

UNCLASSIFIED

UNCLASSIFIED

have been extensively evaluated at temperatures between 76 and 300°K. A supporting program of property measurements includes thermal expansivities, shear and compression modulus, differential thermal analysis, and the force-temperature effects of prestressed elastomers. O-rings and other specimens have been prepared and supplied by Aeronautical Systems Division.

UNCLASSIFIED

UNCLASSIFIED